Optimization of Reactive Ion Etching to Fabricate Silicon Nitride Stencil Masks in SF_6 Plasma

A Thesis

Presented to

the Faculty of the Department of Electrical and Computer Engineering

University of Houston

In Partial Fulfillment

of the Requirements for the Degree

Master of Science

in Electrical Engineering

by

Prithvi Basu

August 2013

Optimization of Reactive Ion Etching to Fabricate Silicon Nitride Stencil Masks in SF_6 Plasma

Prithvi Basu

Approved:

Chair of the Committee
Paul Ruchhoeft, Associate Professor
Electrical and Computer Engineering

Committee Members:

Dmitri Litvinov, Professor
Electrical and Computer Engineering

Richard C. Willson, Professor
Chemical and Biomolecular Engineering

Suresh K. Khator, Associate Dean
Cullen College of Engineering

Badri Roysam, Professor and Chair
Electrical and Computer Engineering

Acknowledgements

I would foremost like to thank my advisor, Dr. Paul Ruchhoeft, for all his guidance and support towards the completion of my master's degree. I would also like to thank Carmen Pascente, Gauri Samel, and David Shakarisaz for being excellent lab mates and their invaluable advice on numerous problems. I would also like to acknowledge Azeem Nasrullah, Tim Sherlock, and Jon Elizalde for all of their training and assistance during the initial stages of my research. Finally, I would like to thank my parents: Bhaskar Basu and Shikha Basu for many years of both emotional and financial support.

Optimization of Reactive Ion Etching to Fabricate Silicon Nitride Stencil Masks in SF_6 Plasma

An Abstract

of a

Thesis

Presented to

the Faculty of the Department of Electrical and Computer Engineering

University of Houston

In Partial Fulfillment

of the Requirements for the Degree

Master of Science

in Electrical Engineering

by

Prithvi Basu

August 2013

Abstract

Stencil masks are used to print ultra-high resolution patterns using helium ion/atom beam lithography and are often manufactured from thin, free-standing silicon nitride membranes. The masks have sub-200nm openings etched through the thickness of the membrane using a reactive ion etch (RIE) process that determine the printed pattern. This project deals with the optimization of a sulfur hexafluoride and oxygen RIE. In this process, 0.5μm thick silicon nitride membranes are coated with 20nm of copper (hard mask) and 200nm of poly (methyl methacrylate) (resist). The desired patterns are then formed in the resist by electron beam lithography, and the patterns are transferred through copper by argon milling. A mixture of 0.8 millitorr of sulfur hexafluoride and 0.2 millitorr of oxygen is used in an RIE step at a power of 15 watts to transfer them through the thickness of the membrane. The process allows for the patterning of extremely straight features (anisotropic etch), has excellent selectivity (200) between silicon nitride and copper, suffers from minimal RIE lag, and is generally very robust. The challenges associated with this process lie in etch non-uniformity due to membrane heating and pattern fidelity in the milling step. Solutions to these problems have been explored and stencil masks with sub-200 nm etched openings have been successfully fabricated.

Table of Contents

List of Figures

List of Tables

Chapter 1 Introduction and Background

1.1 Ion Beam Proximity Lithography

Ion beam proximity lithography is a low cost, high throughput printing technique capable of printing sub 100nm features in a laboratory with minimal hardware requirements. In proximity lithography, the gap between the resist and the mask is very small, whereas in projection lithography, the mask image is projected at a distance from the mask. Projection lithography requires extremely expensive and complicated hardware and equipment which may not be feasible with a laboratory set up at a university. Ion proximity lithography, on the other hand can be operated with equipment at a reasonable cost and hence far more user friendly in a university laboratory set up. In ion proximity lithography, ions that are extracted from a source, drift through a beam line to an exposure station, and illuminate a mask that defines the pattern through the transmission openings in a stencil mask. After passing through the membrane openings, the ions are used to print the desired pattern on the substrate.

Ions are particles with net electrical charges, which usually are atoms lacking one or more orbiting electrons. Therefore, they can be steered by electric or magnetic fields. A collimated beam of energetic ions irradiates a mask placed in close proximity to a substrate coated with an ion sensitive resist. Ions are well suited for lithography because they suffer little or no scattering in the resist unlike electrons. Ion proximity lithography operates under vacuum and uses ions instead of photons to expose the mask features onto a resist coated wafer. A

simple diagram of how this works is shown in Figure 1.1. The ions produce secondary electrons as they travel through the resist, causing chemical reactions that alter the solubility of the resist in the regions of exposure. For positive tone resists, the secondary electrons cause chain scission events that decrease the molecular weight of the resist polymers and increase the solubility. For negative tone resists, the secondary electrons cause cross-linking events that increase the molecular weight of the resist molecules and decrease the solubility.

Energetic ions have a very low wavelength and, unlike photons, suffer from very little diffraction effects at the nanometer scale. The ion source is an important component of ion proximity lithography. Its performance determines many of the parameters of the beam downstream. The main resolution limitations of proximity lithography are ion scattering at the mask, ion scattering in the resist, and penumbral blur. Using thick stencil masks and thin resist layers, ion scattering events can be minimized and penumbral blur becomes the main resolution limitation [1]. One of the most important features of ion proximity lithography is that its ions have extremely small particle wavelengths (for instance, the de Broglie wavelength of 100 keV He^+ ions is just $5x10^{-5}$nm). Whereas photon-based optical lithography or EUV lithography is operated at the diffraction-limited resolution at which the shortest wavelength currently considered is on the order of 3.5 nm in the EUV region.

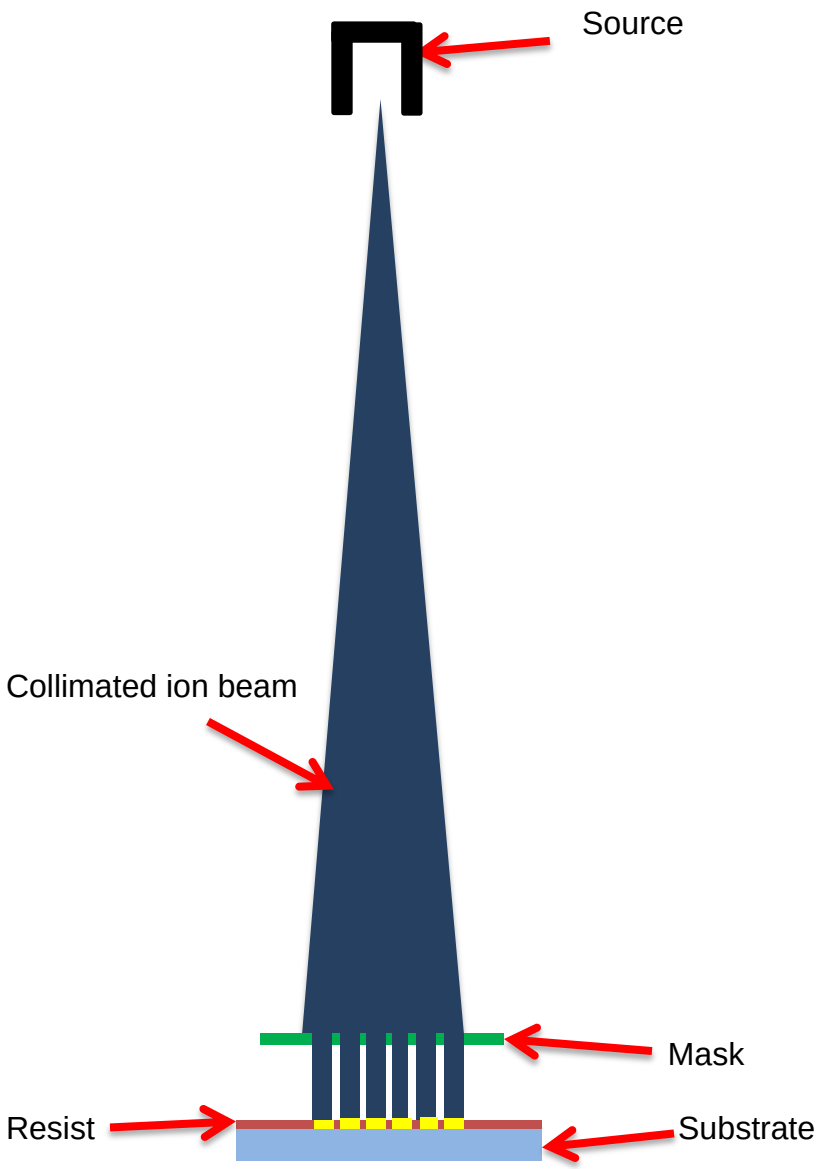

Figure 1.1: Schematic diagram of how ion beam proximity lithography works.

In general, for particle-based optics, one requires that the diffraction-limited resolution should be one tenth of the minimum feature size to be printed [1]. Moreover, ions possess advantages over other high energy particles used in nanofabrication. For example, when compared to electrons, ions are much

heavier and can strike with greater energy at relatively shorter wavelengths to directly transfer patterns onto hard materials (such as semiconductors, metals, or ceramics) without major forward- and back-scattering. Thus the feature size of the patterns is largely dictated by the beam size and the interaction of the beam with the target material. Moreover, the lateral exposure in an ion beam is very low, thereby exposing only the correct areas and writing very narrow lines in the substrate, which makes it more capable to directly fabricate nanostructures.

1.2 Scope of the Project

The emphasis of this project is to develop a robust and reproducible process for forming stencil masks with sub-200nm feature sizes. Stencil masks consist of thin silicon nitride membranes with openings of sub-200nm features that allow ions to pass through them and print a pattern on the substrate. The first approach that was used to make stencil masks of silicon nitride was using a wet etch technique that consisted of using copper as the hard mask which had PMMA (poly (methyl methacrylate)) on it as the resist. The first step was the pattern transfer into the copper using citric acid as the copper etchant followed by reactive ion etching into the silicon nitride membrane using sulfur hexafluoride (SF_6) and oxygen. However, due to certain drawbacks of the wet etch technique, this process was deemed unreliable and dry etching was used as an alternative. The dry etching consisted of an argon milling process where the copper was milled in argon for the pattern transfer in the hard mask, followed by reactive ion etching into the silicon nitride membrane using SF_6 and oxygen. The etch rate

characterization was also very important, as it told us how long to run each of the individual processes.

Chapter 2 is a literature review of plasma etching, including reactive ion etching and sputtering. Also the concepts of selective etching and the anisotropic nature of etching are also discussed. Another literature review of stencil masks follows these where previous techniques and methods for mask fabrication is discussed in details. Chapter 3 describes the main tools used in this project, namely the thermal evaporator and the reactive ion etcher. Their individual components and working principle have been described and pictorially presented. Chapter 4 deals with the stencil mask fabrication processes that have been introduced to in the previous paragraph. Chapter 5 is about optimizing the ideal conditions for the project, where experiments were carried out and data were collected to plot graphs in order to give us a clear indication about what should be the optimum conditions for the project. Chapter 6 summarizes the document and concludes this research project.

Chapter 2 Plasma Etching and Stencil Masks: Literature Review

Anisotropic profiles and line widths as small as 50 nm have been controllably achieved using pattern transfer by dry etching through stencil masks. Plasma etching was introduced in the seventies, mainly for stripping resists. In the eighties, plasma etching became a mature technique to etch layers and was introduced in the production of integrated circuits. Reactive Ion Etching (RIE) was the main technology, but new techniques were developed. An important feature of RIE is its ability to achieve etch directionality. In the nineties new techniques of reactive ion etching, such as electron cyclotron resonance (ECR), and inductively coupled plasmas (ICP), were introduced, with mixed success.

Plasma is a (partially) ionized gas. In the plasma, free electrons collide with neutral atoms/molecules and, through a dissociative process, they can remove one electron from the atom/molecule, which gives a net result of 2 electrons and 1 ion. Depending on the energy of the incoming electron, this collision can result also in other species, such as negative ions, because of electron association, excited molecules, neutral atoms and ions. The light emitted by the plasma is due to the return of excited electrons to their ground state. As the energy between the electron states is well defined for each element, each gas will emit light at specific wavelengths, which will give us the possibility to analyze the plasma. Capacitatively coupled RF plasmas are still the most common plasmas used in dry etching. A typical reactor chamber is shown in Figure 2.1. The power is applied to the lower or the upper electrode (or in some

special cases to the reactor walls). In general the frequency of the applied power is 13.56 MHz. A so-called dark sheath is formed in the neighborhood of all surfaces in the reactor, electrodes and wails. This dark sheath can be considered as some kind of dielectric or a capacitor. So it can be assumed that the applied power is transmitted to the plasma through a capacitor.

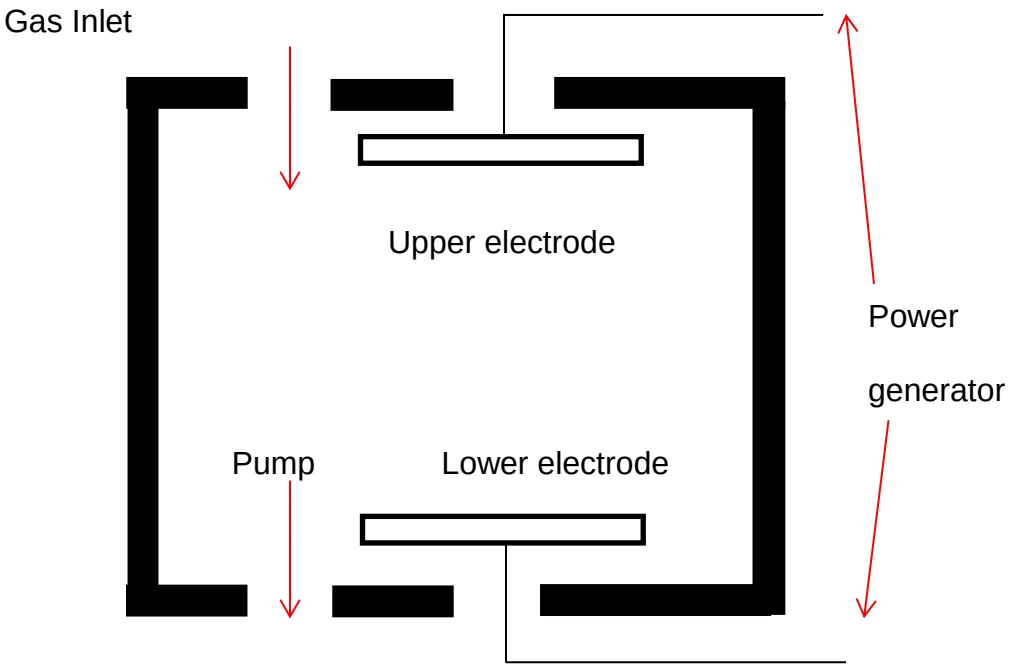

Figure 2.1: Schematic diagram of plasma etch reactor.

At frequencies between 1 MHz and 100 MHz, the free electrons are able to follow the variations of the applied electric field and, unless they suffer a collision, they can gain considerable energy, of the order of some hundred electron volts. On the other hand, in this frequency range, the movement of the much heavier (positive) ions is very little influenced (one may simplify that they are not influenced) by these electric fields: their energy comes completely from

the thermal energy of the environment and is of the order of a few hundredths of an electron volt. In the pressure range of these plasmas, from a few millitorr to a few hundreds of millitorr, the electrons will travel much longer distances than the ions, and in this way, they will much more frequently collide with the reactor walls and electrodes and consequently be removed from the plasma. As they leave the plasma, it becomes positively charged. However, plasmas remain neutral. Because the electrons have a very high mobility compared to positive ions, it is impossible to generate a high positive bias on a surface in contact with plasma. The negative potential between the plasma and a surface can be increased by applying an externally generated negative potential to the surface. This applied potential can be in the form of a continuous Direct Current (DC), pulsed DC, alternating current (AC) or radio-frequency (RF) potential.

2.1 Reactive Ion Etching

The basis of plasma-assisted etching is simple: use a gas glow discharge to dissociate and ionize relatively stable molecules forming chemically reactive and ionic species and choose the chemistry such that these species react with the solid to be etched to form volatile product. A glow discharge is generated from a suitable feed gas (e.g., SF_6) by electron-impact dissociation/ionization the gas phase etching environment which consists of neutrals, electrons, photons, radicals and positive and negative ions. In the plasmas, free electrons collide with neutral atoms/molecules and, through a dissociative process, they can remove one electron from the atom/molecule, which gives a net result of two

electrons and one ion [7]. Depending on the energy of the incoming electron, this collision can result also in other species, such as negative ions, because of electron association, excited molecules, neutral atoms and ions.

The wafer is placed on a radio frequency driven capacitatively coupled electrode. Since the electron mobility is much greater than the ion mobility, the electrons frequently collide with reactor walls and electrodes and they leave the plasma. This leaves the plasma positively charged and a DC electric field is formed that prevents further electrons from leaving the plasma. The potential that appears at the surface of the driven electrodes in a parallel plate arrangement depends on the relative areas of the electrodes. This potential is the D.C. self-bias potential. Positive ions from the glow region are forced to the substrate surface by way of the D.C. self-bias and will assist the etching. Radio frequency driven electrode surfaces immersed in plasma assume a self-bias with respect to ground. This bias depends strongly on the electrode configurations and the capacitance in the circuit. For the case of the symmetric RF system, where the electrodes are of equal area and there is no capacitance in the circuit, the plasma potential is slightly more positive than the positive electrode. If, on the other hand, the electrode areas are unequal in size, there is a capacitance on one branch of the external electrode circuit and the RF circuit is asymmetric. In the asymmetric discharge, the electrode having the smaller capacitance (e.g., smaller area) has a higher negative potential with respect to plasma than the other electrode and it is bombarded with higher energy ions.

The reactive radicals adsorb on the Si surface. This step can be simply controlled by the diffusion of the reactive species to the surface. A reaction between the adsorbed species and the Si must take place. In the case of fluorine-based etching of Si, a chemical reaction between the fluorine atoms and the surface produces spontaneously either volatile species or their precursors. The desorption of the reaction product into the gas phase requires that the reaction product is volatile, thus it should have a high vapor pressure at the substrate temperature. Additionally, there should be no deposited blocking film at the surface. The removal of these films can be greatly accelerated by ion bombardment via sputtering. The desorbed species diffuse from the etching surface into the bulk of the plasma and should be pumped out, otherwise plasma-induced dissociation of product molecules will occur and re-deposition can take place [11]. A schematic diagram of the RIE set up is shown in Figure 2.2.

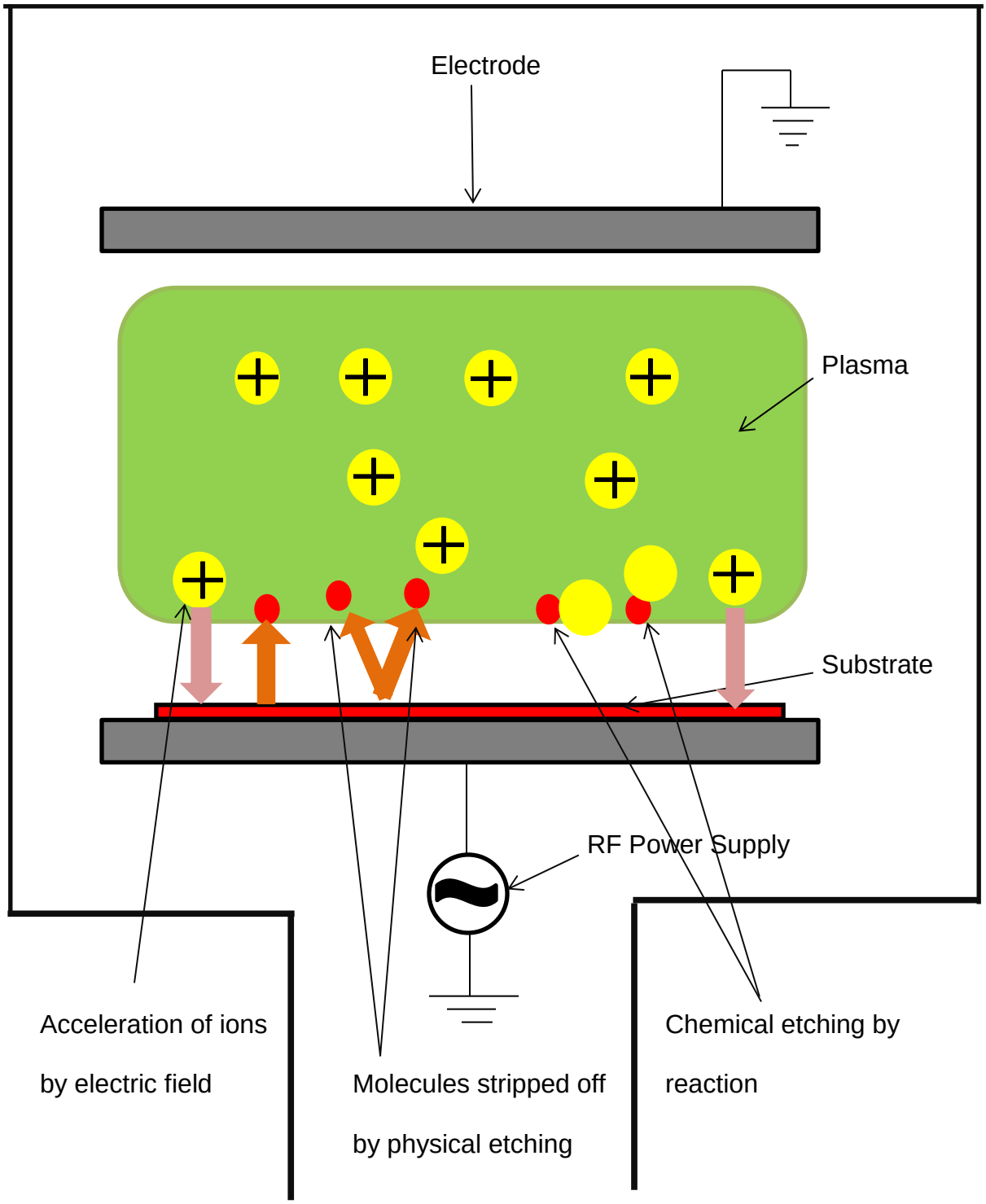

Figure 2.2: Simple diagram of RIE process.

Ion-enhanced or ion-assisted etching can be divided in two main groups: Energy-driven ion-enhanced etching and Inhibitor ion-enhanced etching [11].

Energy-driven ion-enhanced etching: A synergistic effect of ion bombardment in the presence of reactive neutral species leads to removal rates that exceed the sum of separate chemical etching and sputtering rates. The energetic ions damage the surface and leave the material more reactive toward incident neutrals. This process offers highly anisotropic features.

Inhibitor ion-enhanced etching: The role of ions in this mechanism is to clear the inhibitor from the horizontal surfaces. The protective film is not removed from the vertical walls because only a few scattered ions strike these surfaces. This protective film may originate from polymer-like forming precursors that adsorb during etching or from non-volatile etch products. This process, if properly controlled, can develop anisotropic features over very large etch depths.

2.2 Sputtering

Sputtering, also known as sputter etching, is used for patterning surfaces, for cleaning surfaces, and for a number of applications which require careful, microscopic erosion of a surface. Sputtering occurs whenever any particle strikes a surface with enough energy to dislodge an atom from the surface. The sputter yield is just the ratio of the number of emitted particles per incident particle.

Sputtering can occur for most incident species, including atoms, ions, as well as molecules and molecular ions. For virtually all practical cases, sputtering almost always utilizes ion bombardment, either with inert gas ions such as Argon.

The incident particle impacts the surface or near-surface atoms of the solid with sufficient energy to break bonds and dislodge atoms. If, during this process, one or more atoms are removed from the solid, they are considered to be sputtered atoms. At incident energies of more than 40 eV, the incoming particle has more than enough energy to dislodge atoms [7]. The collision sequence is erratic, though, and depends on exactly where the incident particle hits. After this first collision, the incident particle and the impacted one move on into the material causing more and more collisions. The nature of these collisions is difficult to follow, though, because it depends on exactly where the first particle hits. Eventually, though, these knock-on collisions may result in an atom at or near the surface being ejected from the solid. The collision cascade is shown in Figure 2.3.

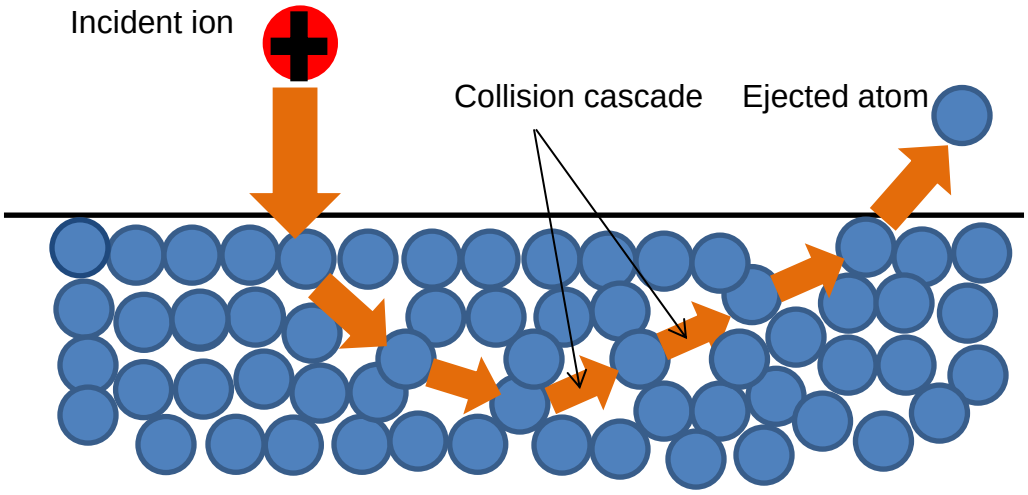

Figure 2.3: Diagram showing collision cascade in sputtering.

The sputtering rate can be however increased by introducing a configuration called a Magnetron configuration [7]. Magnetrons make use of the fact that a magnetic field configured parallel to the target surface can constrain

secondary electron motion to the vicinity of the target. The magnets are arranged in such a way that one pole is positioned at the central axis of the target and the second pole is formed by a ring of magnets around the outer edge of the target. Trapping the electrons in this way substantially increases the probability of an ionizing electron-atom collision occurring. The increased ionization efficiency of a magnetron results in a dense plasma in the target region. This, in turn, leads to increased ion bombardment of the target, giving higher sputtering rates. Figure 2.4 shows the principle of magnetron sputtering.

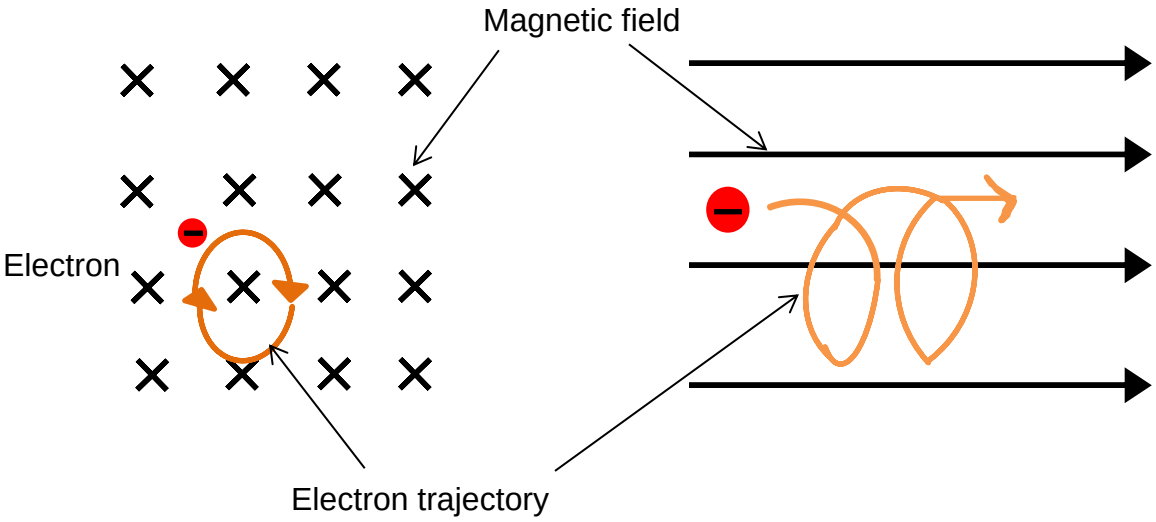

Figure 2.4: Diagram showing principle of magnetron sputtering.

2.3 Selectivity and Anisotropy

Selectivity is a critical etch parameter which refers to the relative etch rate of the film to be etched to the etch rate of another material exposed to the etchant. There are two types of selectivity, one with respect to the masking material and the other with respect to an underlying film. High selectivity with respect to both layers is needed to produce the required pattern resolution with

minimal erosion of the mask and attack of the underlying film and other exposed materials. Figure 2.5 shows an example of selective etching.

Figure 2.5: Example of selective etching between resist, film and oxide.

From Figure 2.5, if R_f is etch rate of nitride film and R_{pr} is the etch rate of photoresist, and then the selectivity of film to photoresist is given by $R_f / R_{pr.}$ Similarly, if R_{ox} is the etch rate of oxide layer then the selectivity of film to oxide is given as $R_f/R_{ox.}$ The key feature of reactive ion etching is its anisotropic nature. Anisotropic etch refers to a process in which etch rate in the direction normal to the surface is much higher than in direction parallel to the surface. Figure 2.6 shows the anisotropic nature. In anisotropic etching the etch suffers from very little to almost negligible undercuts (which is predominant in isotropic etch). The degree of anisotropy as demonstrated in the Figure 2.6 (a) gives us a clear indication of the process. In Figure 2.6, *Z* is the measure of etch in the vertical direction while *X* shows the undercutting associated with it in Figure 2.6 (b). We define the degree of anisotropy, *D*, as

$$D = \frac{Z - X}{Z}. \quad (1)$$

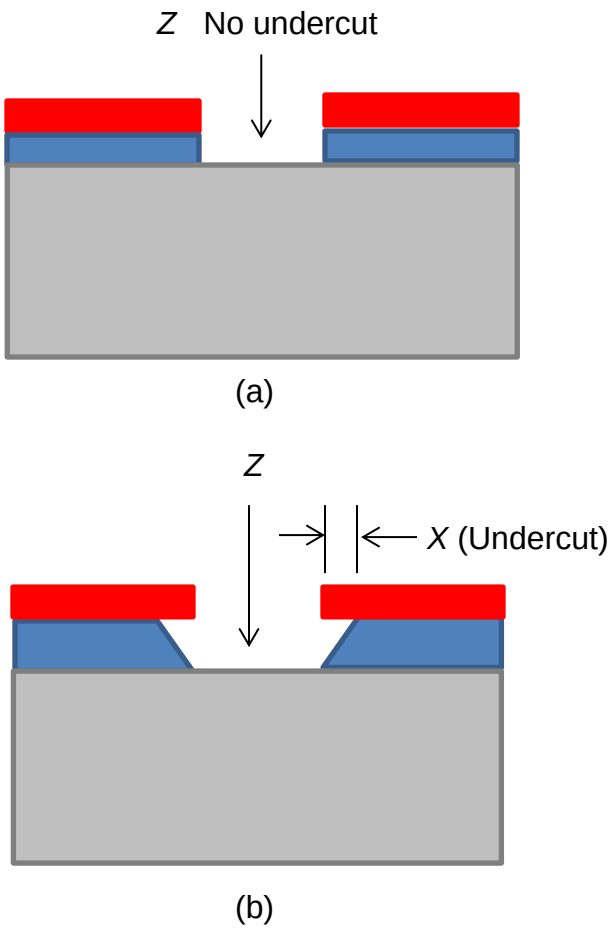

Figure 2.6: Diagram explaining the degree of anisotropy in an anisotropic etch.

In Figure 2.6 (a), *D* is 1, while in Figure 2.6 (b), *D* is slightly less than 1.

2.4 Stencil Masks

Stencil masks of non-stoichiometric silicon nitride (SiN_x) generally consist of a thin silicon nitride membrane of around 0.5μm to 1μm thickness with transmission holes etched through the entire membrane thickness. In the previous works, masked ion beam lithography (MIBL) using silicon nitride stencil masks at a 25μm mask-to-sample gap had been used to replicate 80nm lines

and spaces in PMMA [1]. The 1µm thickness is sufficient to stop protons and SiN_x stencil masks which were 0.5µm thick were also suitable for stopping protons or helium ions. The most critical phase of mask fabrication is the reactive ion etching step which creates the transmission holes in the silicon nitride. Highly anisotropic etching is required to produce fine transmission patterns in films thick enough to stop energetic ions [2]. Etched profiles with nearly vertical sidewalls are necessary to minimize the scattering of ions through the edges of the transmission holes. Figure 2.7 shows a schematic diagram of a stencil mask.

In earlier work, reactive ion etch process for the SiN_x material used CF_4 as the etch gas with a 250 V self-bias potential. This process is used to etch a 320 nm-period grating through a 1µm thick SiN_x membrane. In this process around 80 nm of nickel was deposited as the hard mask by the lift off technique using x-ray lithography [5]. However the etch profile seen was isotropic since ions could easily be scattered through the non-vertical edges of the transmission hole and could have reduced the mask contrast. Later another RIE process was developed to etch the membrane which used CHF_3 as an etch gas and a 500 V self- bias potential [6].

There were, however, several difficulties with this RIE process. The etching of very fine geometries (that is less than 0.3µm line width) into a 1µm thick film left a 10nm to 40nm thick polymer layer at the bottom of the transmission holes at the SiN_x-Si interface. This layer was not removed by continued etching with CHF_3 and also survived the subsequent mask fabrication steps. This layer was due to polymer deposition [3] which was known to occur in

RIE processes which employ CHF_3. When the etching process reached the membrane interface, the slow etch rate was found to be dominated by the deposition rate of the polymer.

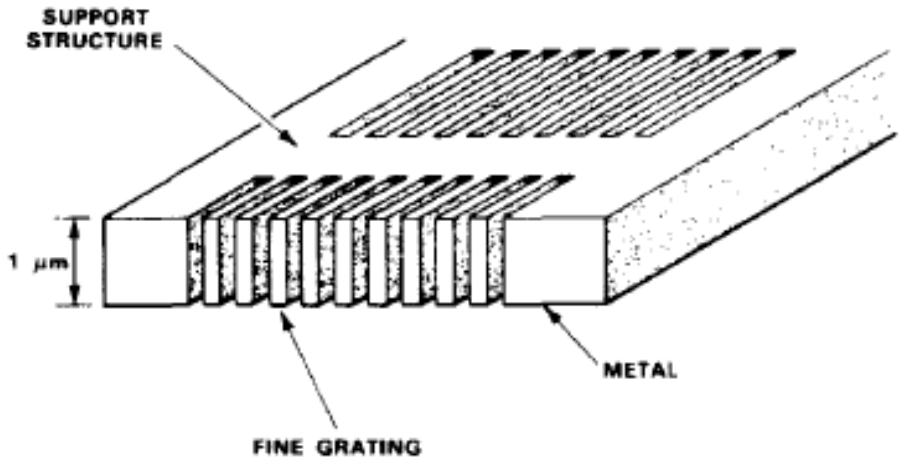

Figure 2.7: Schematic diagram of a stencil mask, taken from ref. [3].

It was discovered that an additional RIE step with CF_4 would have removed this film without significantly affecting the profiles of the transmission holes. Another complicating factor is that for small transmission holes the etch rate decreased as the depth of the hole increased [4]. All these factors led to several incompletely etched masks being carried through the entire fabrication process. The maximum aspect ratio that was achieved was approximately 6:1; therefore masks with 80nm line-widths were fabricated from 0.5μm thick membranes.

Another technique previously used to make stencil masks used palladium as the hard mask [10]. In that process, a double side polished silicon wafer was

coated with 250 nm non-stoichiometric silicon nitride on both sides. A pattern of windows was etched through the silicon nitride on one side of the wafer using a magnetically enhanced reactive ion etching system (MERIE) using 0.8mTorr carbon tetra fluoride (CF_4) + 0.2mTorr Oxygen plasma and 85W power and 250 nm thick free standing silicon nitride membranes were made [10]. A palladium (Pd) layer (20nm) was then deposited on the membrane wafer using dc magnetron sputtering at a base pressure of 10μtorr and an argon (Ar) gas pressure of 10mTorr, followed by spin coating of 60nm of FOX-12 (flowable oxide from DOW Corning). The wafer was then baked at 250ºC to obtain a uniform layer of silicon oxide. The reason for depositing a metal and an oxide layer is to effectively help transfer the resist pattern into the nitride membrane. PMMA (200nm) was then spun on, and the desired pattern was printed using a modified scanning electron microscope as an electron beam writer. The process flow diagram is shown in Figure 2.8.

After patterning, the resist was developed in a room temperature 3:1 solution of isopropyl alcohol (IPA): methyl isobutyl ketone (MIBK) for 45 sec, rinsed in IPA for 30 sec and dried in nitrogen. The resist pattern was first transferred into silicon dioxide using 0.7mTorr of trifluoromethane (CHF_3) gas at 70W power [10]. An argon ion-milling step further transfers the pattern into the thin Pd layer, the hard-mask for transferring the pattern into silicon nitride membrane. It should be emphasized here that the choice of metal layer (as a hard mask) to transfer the pattern into the nitride in the final step is extremely important.

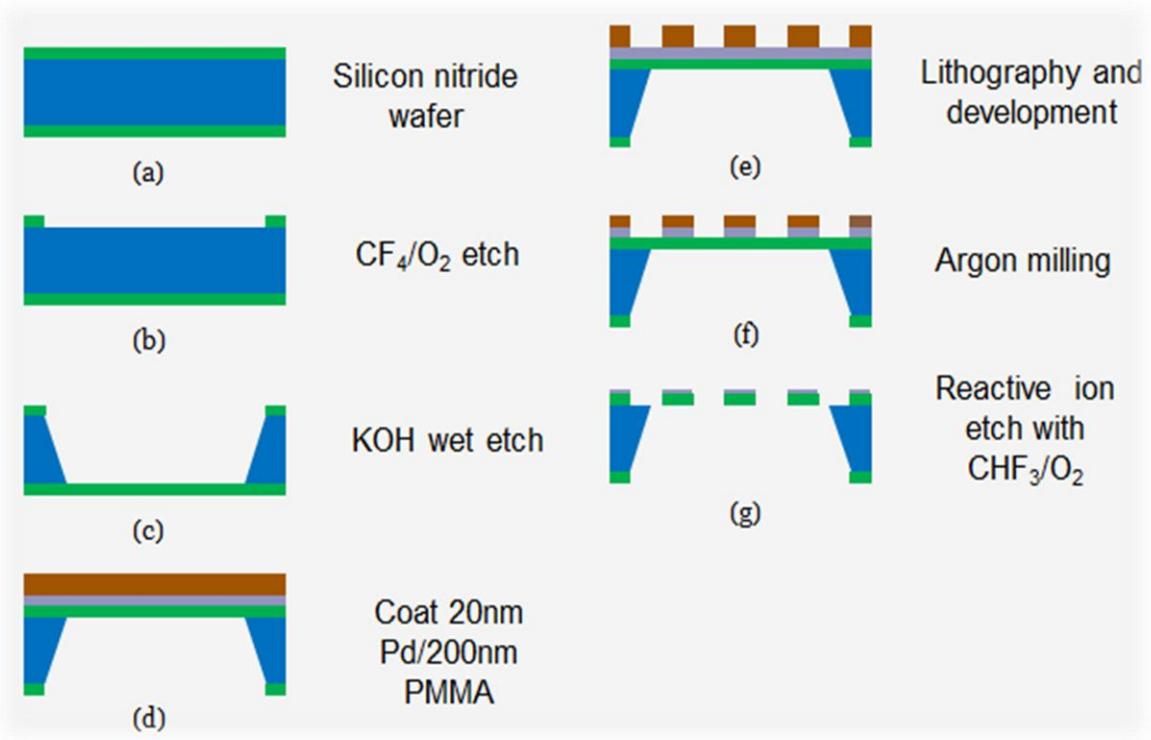

Figure 2.8: Mask fabrication process flow using palladium and PMMA.

Although easily removed by Ar milling, it was found that adding CF_4 dramatically suppresses the milling rates, likely due to the passivation of the Pd surface. Significantly, CF_4/O_2 RIE is a high-rate, anisotropic RIE chemistry for etching silicon nitride. In CF_4/O_2 RIE, Pd etches 150 times slower than the nitride, thus allowing the pattern to be transferred through the entire thickness of the silicon nitride membrane with minimum damage to the palladium hard-mask. For comparison, gold is removed about 20 times faster than palladium in CF_4/O_2 RIE, while the gold/palladium removal rates are similar in argon. That's why palladium was chosen instead of gold as the hard mask as it etches slowly in CF_4.

However, SiN_x stencil masks had their drawbacks too. Thermal distortions in stencil masks were caused by mask heating due to the impinging ion beam [3]. Because the stencil masks are in vacuum, there was no convection cooling. Even if the mask material was a good thermal conductor, such as silicon, the large areas of practical stencil masks compared to their relatively small thickness made conduction a poor method of removing heat and caused thermal gradients across the mask. Because of no convection and poor conduction, radiation cooling is non-negligible in stencil masks. Grid-support stencil masks [2], which employ a matrix of small transmission holes instead of completely open transmission areas, were used to eliminate most of the pattern restrictions associated with stencil masks, and to improve mask stability. Figure 2.9 shows a grid support stencil mask [2]. To fabricate grid-support stencil masks [2], nickel was deposited using lift-off and the combination of the nickel layer together with 300nm of PMMA [2] as the photoresist comprised the mask for the RIE for the transmission holes.

The RIE step used CHF_3 as the etch gas at a self-bias potential of 500V. A tetra-methyl-ammonium-hydroxide (TMAH) etchant was used to remove the silicon from behind the mask membrane in these window areas. The silicon oxide layer was removed with HF solution. Finally a 20nm thick Nickel layer was deposited to prevent charging during exposure. Holes etched in membranes usually resulted in local variations in stress and therefore create pattern-induced distortions. These grid-support stencil masks [2] eliminated local and global

pattern-induced distortion. In these types of structures, high anisotropic etching of high aspect-ratio holes was formed in the membrane.

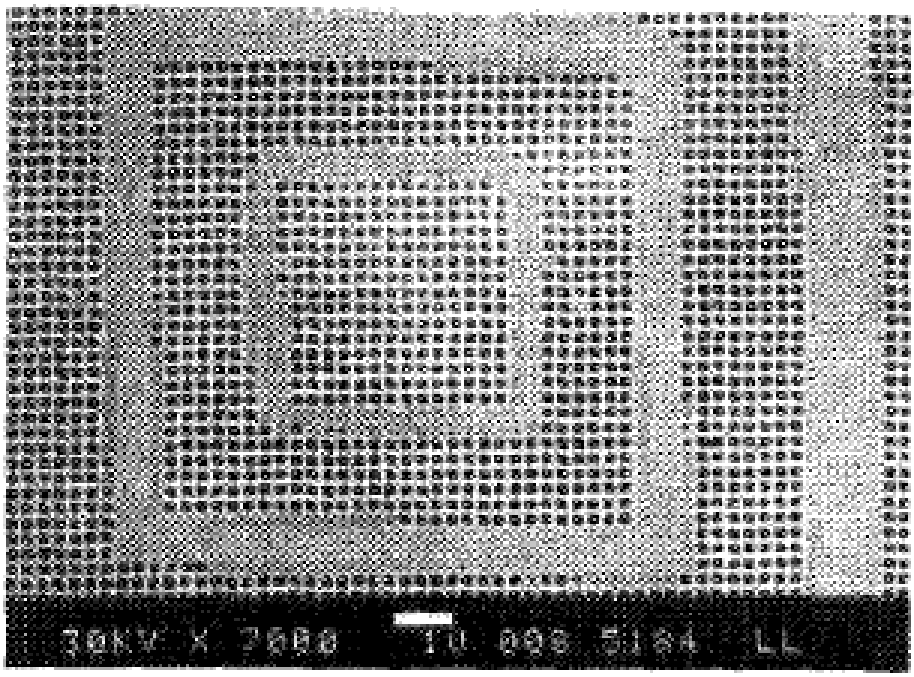

Figure 2.9: Diagram of a grid support stencil mask, taken from ref. [2].

The completely uniform array of holes allowed the stress in the masks to be increased, which subsequently allowed the mask to be stiffer and more resistant to deformation as a result of external perturbation. The use of a grid support mask [2] removed the pattern restrictions usually associated with stencil masks but the highest resolution and most precise line-width control still was obtained with simple stencil masks. Figure 2.10 shows the steps of fabricating a grid support stencil mask [2].

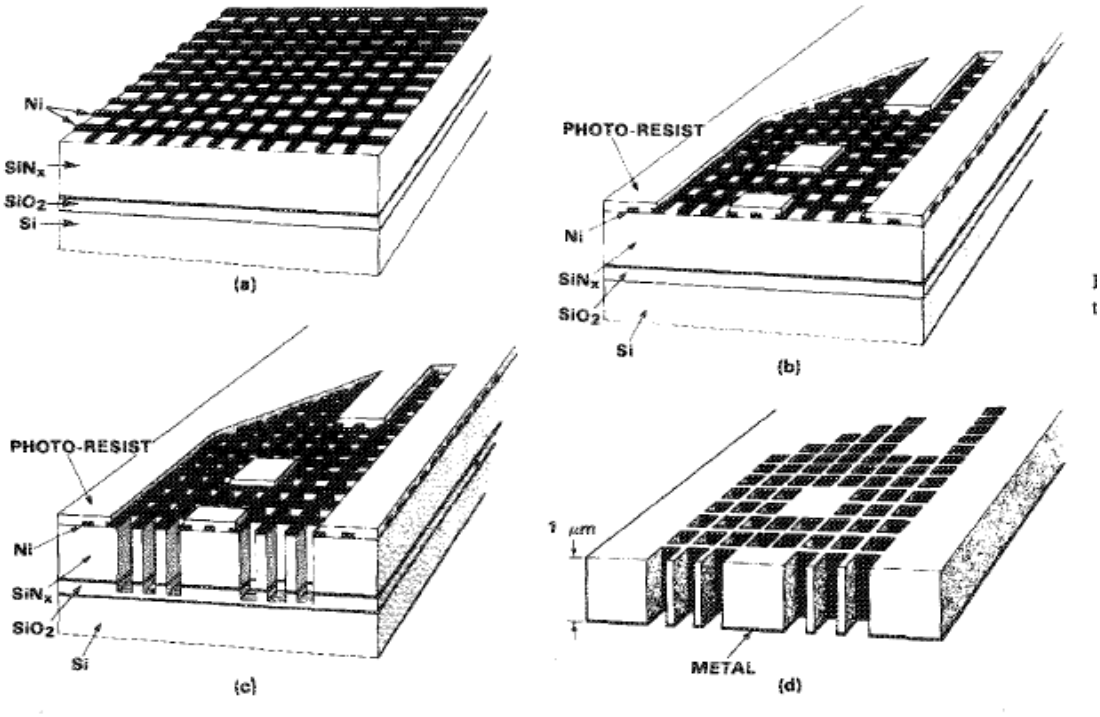

Figure 2.10: Fabrication of a grid support stencil mask, taken from ref. [2].

One major issue was that ions usually impinged [5] on the mask near the perimeter of a transmission hole and scattered laterally in the mask and escaped the mask through the sidewall of a transmission hole at an arbitrary angle. Any ion impinging very near a transmission hole may scatter laterally into the transmission hole and escape the mask at an arbitrary angle. These scattered ions reduced the effective contrast of the mask [4]. This scattering effect produced a background exposure, which results the resist between the exposed lines to slowly develop, both thinning the resist and removing resist from the sides, thus increasing the line-width. Effective contrast [4] in an ion beam stencil mask was defined as the ratio of the total incident ion flux (including ions which

pass through transmission holes) to the flux of ions which strike but escape the mask. From the line-width data that were found it was clear that for simple stencil masks the contrast was not infinite, but large. For grid-support masks [2], however, the situation was considerably different. The area of mask near transmission hole perimeters was significantly increased in grid-support masks [2]. Therefore, a greater amount of ion scattering from this type of mask was expected. Figure 2.11 shows the scattering effect of ions. It was clear from Figure 2.11 that a mask whose thickness is similar to the ion range will have scattered ions escape while a thicker mask with the same pattern and same ion energy will trap most ions in adjacent regions.

The previous mask fabrication processes as explained in this chapter, mostly used CF_4 and CHF_3 as the etchants. However, as a result of this, the entire process was slow as the etch rates of silicon nitride in CF_4 and CHF_3 were slow. In this project SF_6 was used as the main etchant, which was hypothesized to give a far more robust mask fabrication process. The details of this process are described in the next chapters.

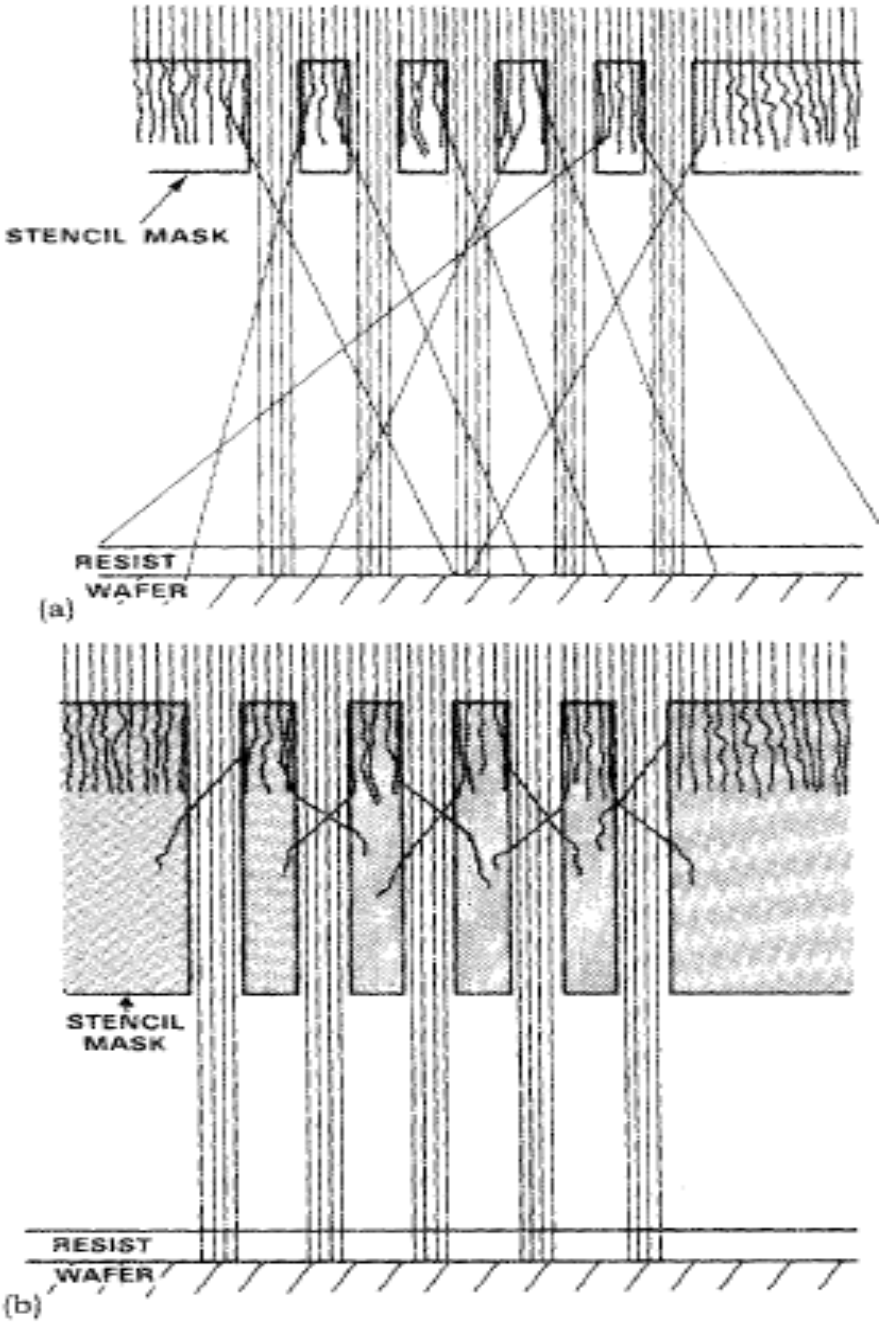

Figure 2.11: Scattering effect of ions in a stencil mask with (a) mask thickness similar to ion range and (b) a thicker mask, taken from ref. [4].

Chapter 3 Fabrication Tools

3.1 Thermal Evaporator

The metals that were evaporated using this tool for this project are 100nm of copper and 100nm of gold. In this process, heat is input into the source material (often called the charge) to create a plume of vapor which travels in straight-line paths to the substrate. Upon arrival at the substrate, the atoms, molecules, and clusters of molecules condense from the vapor phase to form a solid film [9]. The heat of condensation is absorbed by the substrate. On a microscopic scale the localized heating from this process can be enormous. It is common, in the development of metal coating techniques for thin cross-section plastic parts, to melt substrates during the initial deposition runs. The source-to-substrate distances can be selected and deposition rates which will allow coating of temperature sensitive substrates without melting [9]. There are several methods by which heat can be delivered to the charge to cause vaporization: electric resistance heating, induction heating, and electron beam heating [9].

Evaporation of material by electrical resistance evaporation is very likely the easiest of the thermal evaporation techniques. Quite simply, in a vacuum environment the charge (which may be an elemental metal, an alloy, a mixture or a compound) is heated to become a vapor. Low voltage, high current (typically 10 to 40 VDC, 10 to 500 amps) power is brought into the vacuum vessel using electrical power feed through [9]. The electrical power is passed through a

filament is in intimate contact with the charge. Filaments are often heated to 1000 to 2000°C.

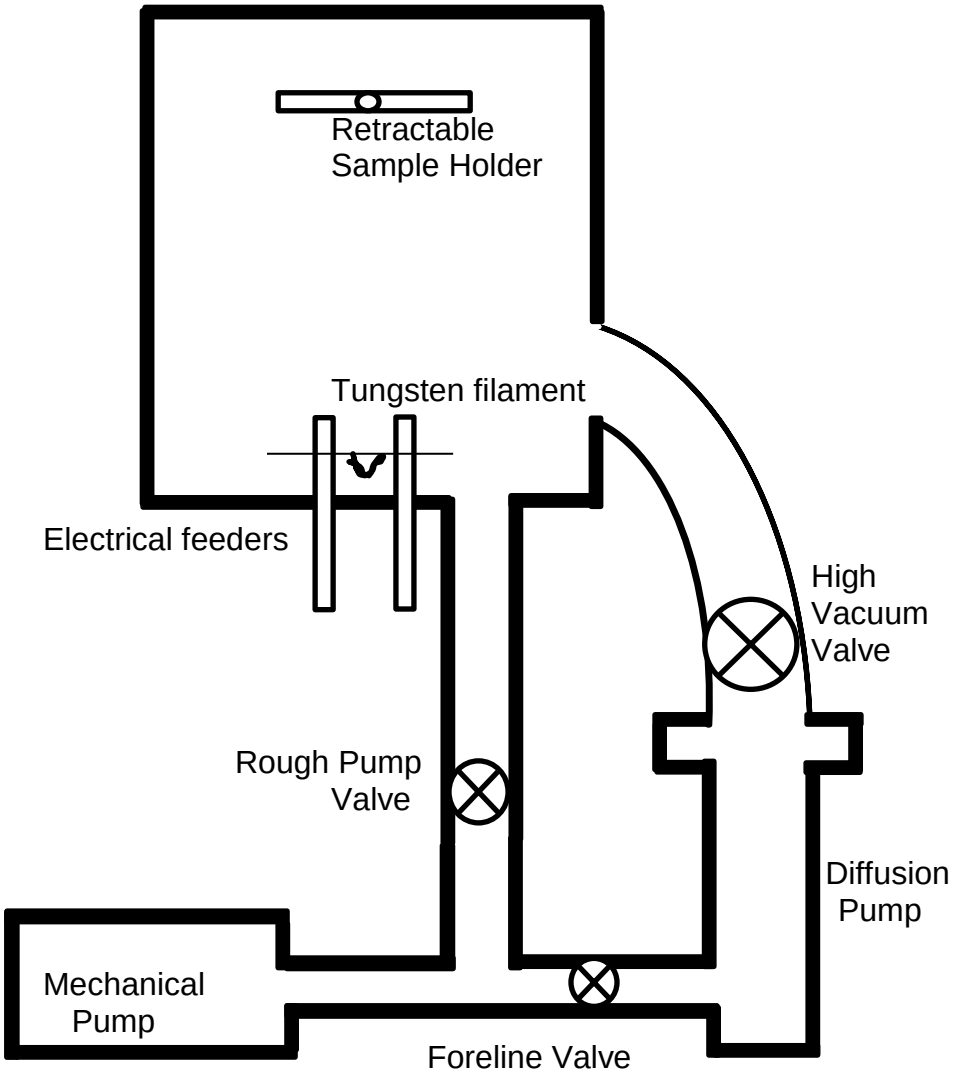

Figure 3.1: Schematic diagram of the thermal evaporator.

A schematic of the evaporator tool is shown in Figure 3.1. As is typical of many vacuum systems, it uses a single rotary vane mechanical pump which

serves to both rough the main vacuum chamber as well as back the high vacuum diffusion pump. To control the pumping, three electrically controlled pneumatic valves are used. The roughing pump valve is between the vacuum chamber and the mechanical pump (backing pump). A vacuum diffusion pump cannot begin its work with full atmospheric pressure inside the chamber. Instead, an ancillary mechanical pump capable of a modest level of pumping first brings the pressure inside the vacuum diffusion chamber down to about 200 mTorr.

The foreline valve is between the diffusion pump and the mechanical pump and the high vacuum valve is between the chamber and the diffusion pump. When the mechanical pump is started for initial pumping the roughing valve is opened keeping the high vacuum valve and the foreline valve closed. When the pressure falls to about 200 mTorr, the roughing valve is closed and the foreline and high vacuum valve are opened and the diffusion pump is turned on. Thus the chamber gets exposed to the diffusion pump and the base pressure of the system reached after pumping is around $2x10^{-5}$ torr. The base pressure was the lowest pressure that the system can attain. Inside the main chamber there are two sets of electrical feed through which allow for the placement of two evaporation sources which can be used sequentially. To measure the deposition rate, a quartz crystal oscillator is used. Finally, a moveable shutter was also added to precisely control the stop and start of deposition on the substrate. To measure the pressure, the system features two thermocouple gauges (one on the chamber, the other on the foreline of the diffusion pump) and a single ion gauge used to measure very low pressure.

3.2 Reactive Ion Etcher

It has all the basic components that the evaporator has: chamber, mechanical pump, diffusion pump. In addition to this it has a gas inlet manifold capable of adding two different gasses to the chamber. It also has an ion gauge to measure the base pressure as well as a Baratron gauge to measure the process pressure. Inside, an electrode is driven with a 13.56 MHz RF signal above the grounded anode plate [9]. This particular design also includes a magnet located below the anode which creates a magnetic field at the substrate. This magnet is placed in this location in order to increase the ion density near the substrate, enhancing the etch rates.

Similar to the thermal evaporator, the reactive ion etcher also operates by the three pneumatic valves: the roughing valve, the foreline valve and the high vacuum valve. The process of operation is exactly similar to the one described in the previous sub-section. The reactive ion etcher was used to etch silicon nitride membranes using SF_6 and oxygen. The argon sputtering step to etch the hard mask was also carried out in this system. The base pressure of the system reached after pumping is around $5x10^{-6}$ torr. The schematic of the etcher tool is shown in Figure 3.2.

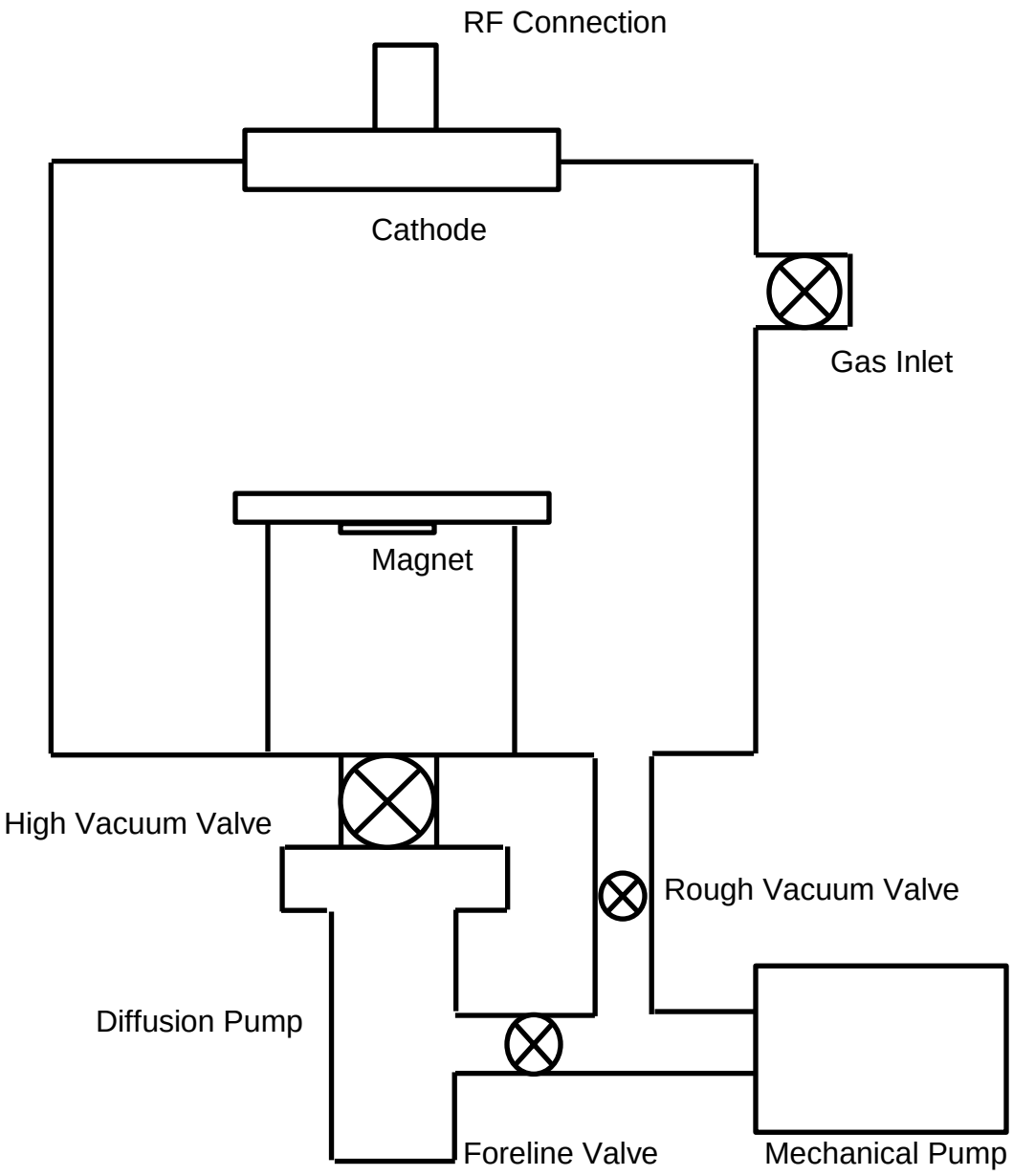

Figure 3.2: Schematic diagram of the reactive ion etcher.

Chapter 4 Stencil Mask Fabrication

4.1 Membrane Formation

Firstly, 0.5 micron thick silicon nitride membranes are formed and additional layers are deposited on a whole wafer. The membranes are formed from double side polished four inch wafers coated with a 500 nm thick layer of non-stoichiometric low stress silicon nitride. Multiple openings or windows of roughly $4cm^2$ size are etched into the silicon nitride layer on one side of the wafer using transparency film as an etch mask. The gasses used are 0.2 mTorr of oxygen and 0.8 mTorr of CF_4 and a power setting of 30 watts.

To form the membranes, the silicon is etched in the exposed windows using a solution of potassium hydroxide (KOH) and water. A large beaker is filled with 2 liters of deionized water and 1 kg of KOH pellets. The wafer is held using a special teflon clamp. The KOH solution is set to 80°C using a temperature probe and stirred at 300 rpm. Once the KOH pellets have completely dissolved, the wafer is placed in the beaker. The etch takes about 8 hours to remove the full thickness of the wafer, and the wafer is kept in the solution another hour to remove any remaining KOH crystals from the membranes. The etched wafer is placed in pure deionized water at 80°C for 30 minutes. The wafer is then placed in room temperature deionized water for 30 minutes. The wafer is placed vertically on a carrier and rinsed with isopropanol, and then drip dried. It is imperative to ensure that no KOH salts are left behind during the rinsing stage on

the membranes or on the wafer frame as the KOH easily crystallizes and it adversely affects our process.

4.2 Wet Etch Process

One of the first techniques of membrane patterning during the mask fabrication process that was tried during the course of this project was the wet etch process. However, the choice of the hard mask is critical in this process and copper was chosen as the hard mask because it can be etched with a suitable liquid etchant, citric acid. In this process, the silicon nitride membrane of 0.5 micron thickness had to be coated with copper and PMMA which is a positive tone resist. After exposing the PMMA to ion/electron beam lithography and developing, the copper had to be etched using citric acid followed by reactive ion etching of the nitride membrane using 0.8 mTorr of SF_6 and 0.2 mTorr of oxygen. The selectivity between silicon nitride and copper in SF_6 was the critical parameter for the etch to be successful.

Before the experiment was performed using the SiN_x membrane, it was carried out on a silicon nitride wafer piece which was 500nm thick. This was a test experiment carried out in order to examine whether the process design works out. The etch rate of copper in citric acid as found out was 33nm per min and the etch rates of copper and silicon nitride in SF_6 and oxygen was 0.13nm per min and 27nm per min respectively. Thus, the selectivity between silicon nitride and copper in SF_6 and oxygen was roughly 200 which were considered sufficiently high for the process to work.

4.2.1 Process Flow of Wet Etch Fabrication

In this process, 10nm of copper was evaporated on the nitride and 70nm of PMMA was spun over the copper. The wafer was then baked at 180ºC for one hour to drive out the solvents from the PMMA. The lines printed were 1 micron lines and they were developed in it is developed in a 3:1 solution of isopropanol and methyl isobutyl ketone and rinsed with isopropanol. The first step consisted of transferring the pattern into the copper followed by RIE of the nitride in SF_6 and oxygen. The process flow diagram of the wet etch fabrication is shown in Figure 4.1.

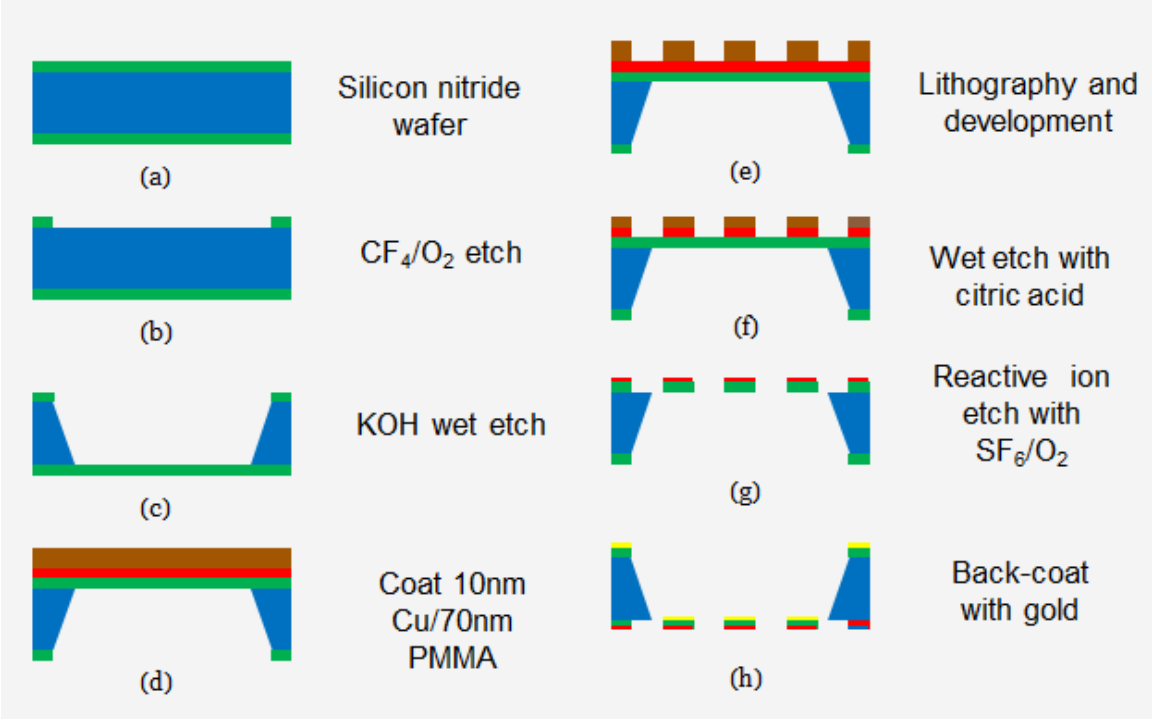

Figure 4.1: Process flow diagram of the wet etch process of mask fabrication using 10nm of copper and 70nm of PMMA.

The back of the membranes were coated with 100nm gold by thermal evaporation. This gold layer serves two purposes: as a conductive layer to prevent charging of the mask and distortion of the ion beam during exposure, and to block ions/atoms from penetrating into the nitride layer and causing a change in stress.

4.2.2 Results and Discussion

Based on the etch rates of copper in citric acid (33nm per minute), the silicon nitride wafer was immersed in the citric acid solution for 18 seconds in order to etch 10nm of copper. Figure 4.2 shows the image of the nitride wafer after 18 seconds of citric acid etch.

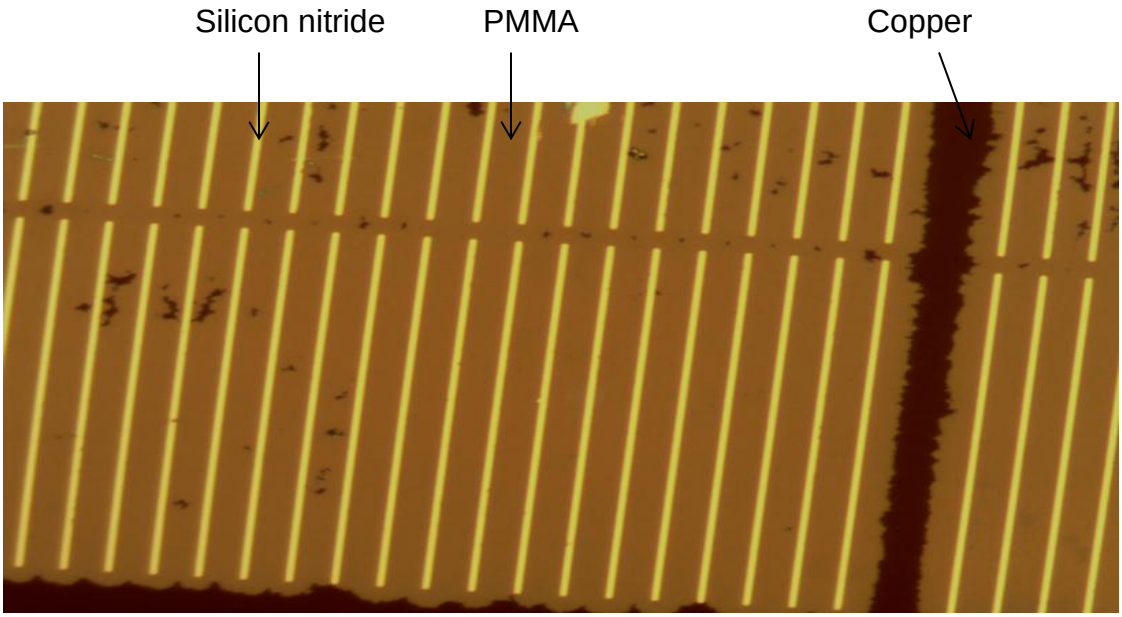

Figure 4.2: Image of silicon nitride wafer after 18 seconds of wet etch in citric acid.

The lines printed on the wafer were 1 micron lines. From the image we see the light brown area around the 1 micron lines, which is PMMA and the dark brown areas are copper. In other words, the PMMA wasn't protecting the copper due to poor adhesion between copper and PMMA or copper and silicon nitride.

4.2.3 Annealing at PMMA Glass Transition Temperature

The next process that was carried out was annealing the PMMA at its glass transition temperature which is 105ºC. Glass transition temperature of a polymer at which, the mechanical behavior of the polymer changes from rigid and brittle to tough and leathery and the behavior we define as plastic behavior. This was done in order to improve the adhesion between PMMA and copper. The PMMA was heated to its glass transition temperature after spin coating on 10nm of copper and baking. This was followed by 5 minutes of citric acid etch to transfer the patterns from PMMA to copper followed by RIE in SF_6 and oxygen for 30 minutes to etch the nitride. The image results after the wet etch for 5 minutes and results after RIE for 30 minutes is shown in Figure 4.3. and Figure 4.4 respectively. From Figure 4.3 it is clear that the 1 micron lines are not straight and a certain degree of roughness exists. These roughness are certainly as a result of poor adhesion between PMMA and copper (or between copper and silicon nitride) during the copper etch and the copper does get exposed and we are losing the vast majority of the copper as a result of that. Even after annealing the PMMA to its glass transition temperature, the adhesion issue was not solved.

From Figure 4.4 (b) and (c), it is seen that after the RIE in SF_6 and oxygen for 30 minutes, there exists a very high degree of roughness in the patterns, showing clearly that even the annealing step couldn't solve the mask failure.

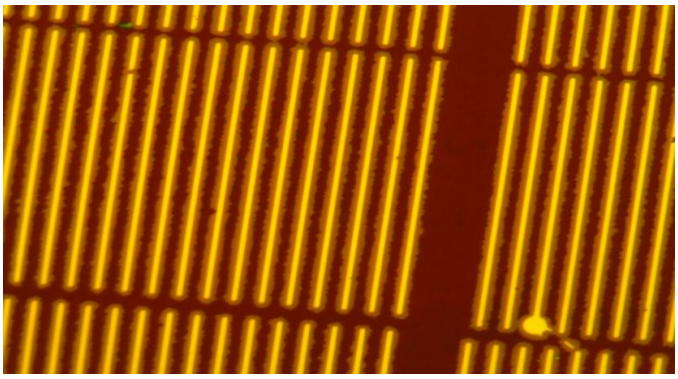

Figure 4.3: Image of silicon nitride wafer after 5 minutes of wet etch in citric acid after annealing PMMA at its glass transition temperature.

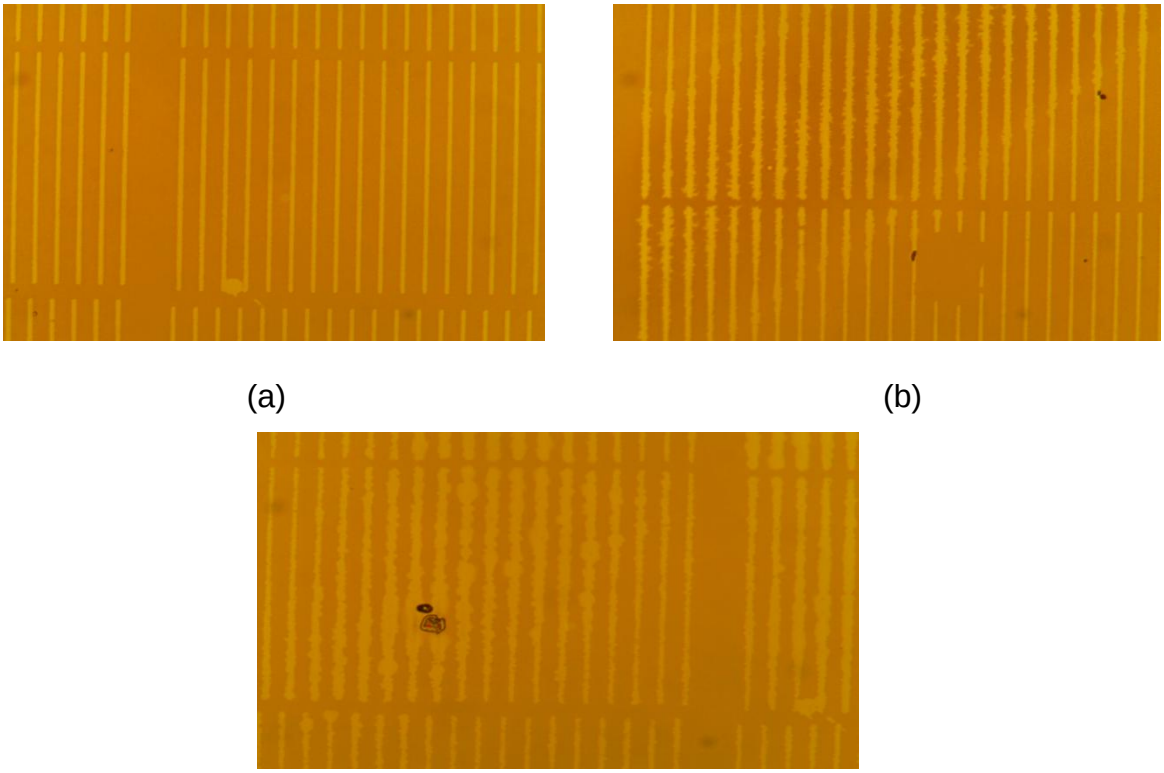

(a) (b)

(c)

Figure 4.4: Images of silicon nitride wafer after RIE in SF_6 and oxygen for 30 minutes.

4.2.4 Conclusion

The wet etch technique consists of three steps: reactant transport to the surface, selective and controlled reaction of the film to be etched, and transport of byproducts away from the surface. Wet etching is a well-established technology but its exact chemistry is incompletely understood. The main drawbacks that affect pattern dimensions and prevent line width control are firstly, poor photoresist adhesion. This is what we experienced in our project which led to the hard mask getting exposed and ultimately led to mask failure. Secondly, the etch is isotropic, which is non-directional removal of material from a substrate via a chemical process using an etchant substance. By non-directional it means that there exists some lateral undercutting and the etch proceeds at the same rate downward as it does laterally in a liquid solution. Figure 4.5 shows the undercuts arising as a result of wet etch. In this figure, W refers to the width of the undercut leading to mask failure. However in our process the thickness of copper (hard mask) was 10nm which was very thin. So we did not experience undercutting to that extent. However the major drawback of the wet etch process was the adhesion issue between PMMA and copper or copper and silicon nitride which led to the conclusion that this process was unreliable in terms of mask fabrication and therefore dry etching was the other alternative.

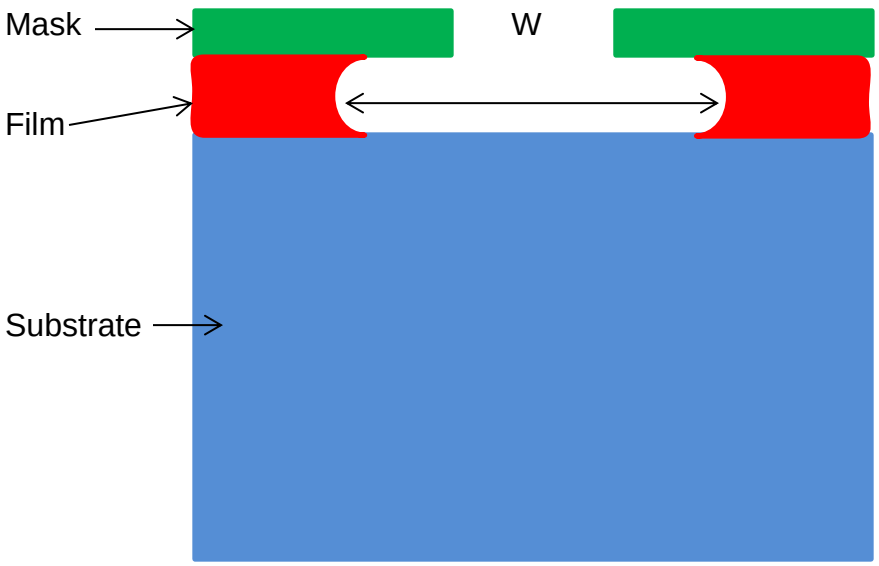

Figure 4.5: Undercutting leading to mask failure due to isotropic etch.

4.3 Dry Etching Technique

The unreliability of the wet etch led to the dry etch techniques for the mask fabrication process. This process chiefly consisted of two etching steps: the first being the argon milling step (or sputtering) to etch the patterns in the hard mask followed by reactive ion etching in SF_6 and oxygen to etch it into the silicon nitride. Previous works have dealt with CF_4 and oxygen, but that process was too slow due to the etch chemistry of CF_4 where a polymer formation took place and subsequently slowed the etch process. In this work however only SF_6 and oxygen were used for the silicon nitride etches. The choice of the hard mask is the key step in this process and also the selectivities between the hard mask and PMMA and also the selectivity between the hard mask and the silicon nitride is also critical for the process to work. The role of the hard mask is that it protects the

silicon nitride below it from getting exposed to the SF_6 and oxygen. That's why we need two pattern transfer processes instead of directly transferring the pattern from PMMA to the nitride. Previously, nickel, chromium, or palladium was used as the hard mask. In our project we used palladium and copper to find out which metal would be used as the hard mask. Table 4.1 and 4.2 shows the etch rate characterization for the pattern transfer into the hard mask (argon milling step) and the etch rate characterization for the pattern transfer into the silicon nitride (SF_6 and oxygen etch) using both palladium and copper respectively.

Table 4.1: Etch rate characterization for pattern transfer into hard mask.

	Palladium	**Copper**	**PMMA**
Selectivity	3	1.46	
Rates(nm/min)	2	4.1	6

Table 4.2: Etch rate characterization for pattern transfer into silicon nitride.

	Palladium	**Copper**	**Silicon nitride**
Selectivity	135	200	
Rates(nm/min)	0.2	0.13	27

The argon milling step was carried out at a process pressure of 1 mTorr and at a power of 13 watts while the RIE of silicon nitride was carried out in 0.8 mTorr SF_6 and 0.2 mTorr of oxygen at 15 watts. Based on the etch rate characterization for the two processes and from the data in Table 4.1 and 4.2, it was clear that copper should be chosen as the hard mask. The reason being the selectivity between PMMA and copper was lower (implying that sufficient PMMA will be left over after the argon milling step) and the selectivity between copper and silicon nitride was much higher than palladium.

4.3.1 Process Flow of Dry Etch Fabrication

In this process, we used 200nm of PMMA and 20nm of copper. Based on the etch rates, the argon milling step was first run for 10 minutes which consumed 60nm of PMMA roughly and covered a 100 percent over etch for the copper. The SF_6 and oxygen etch was run for an hour on a silicon nitride membrane. An hour long etch is roughly a 200 percent over etch of the nitride and leaves behind roughly 10 to 12 nm of copper. The process flow diagram is shown in Figure 4.6.

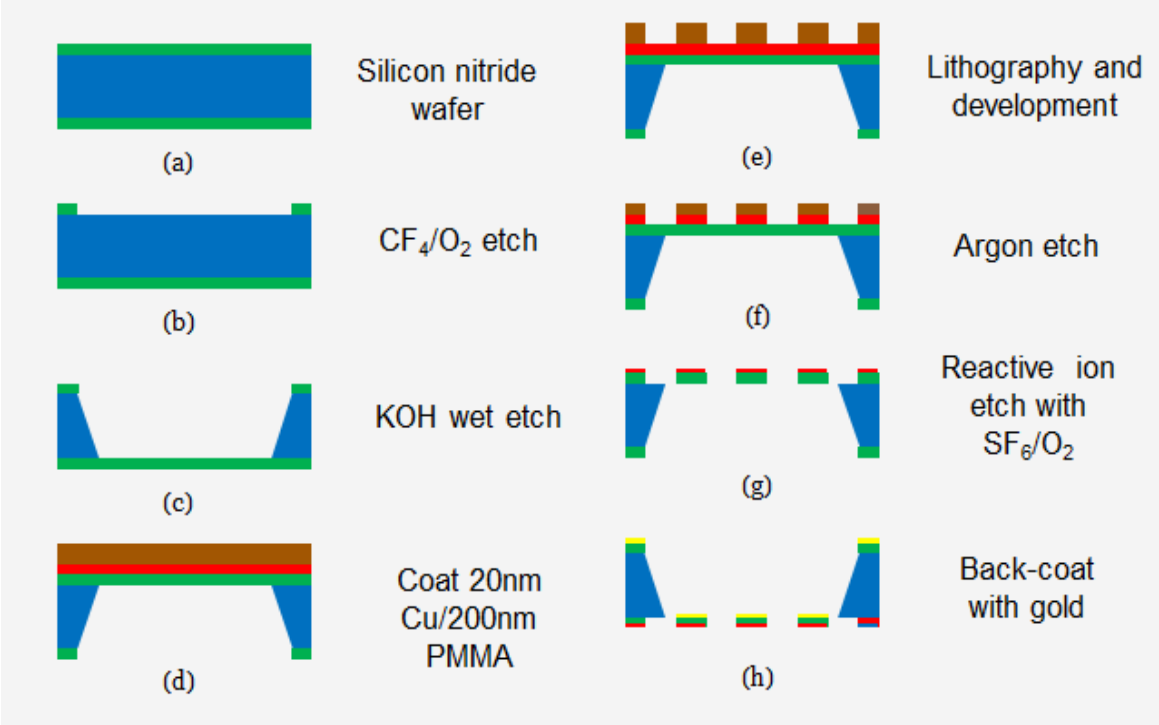

Figure 4.6: Process flow diagram for mask fabrication using dry etch technique using 20nm of copper as hard mask and 200nm of PMMA as photoresist.

The back of the membranes were coated with 100nm gold by thermal evaporation. This gold layer serves two purposes: as a conductive layer to prevent charging of the mask and distortion of the ion beam during exposure, and to block ions/atoms from penetrating into the nitride layer and causing a change in stress.

4.3.2 Etching of Silicon Nitride Membrane

After the membranes were made and coated with 20nm of copper and 200nm of PMMA, patterns ranging from 5 microns to 100nm were printed on the membrane and developed using a 3:1 solution of isopropanol and methyl isobutyl

ketone and rinsed with isopropanol. The first step consisted of etching the patterns into the copper layer by argon milling for 10 minutes followed by reactive ion etching in 0.8 mTorr SF_6 and 0.2 mTorr of oxygen for an hour to etch through the nitride membrane at a power of 15 watts. The reason for this hour long etch for a membrane is largely due to the fact that the membrane gets heated up due to its poor thermal conductivity and so the etch slows down. To overcome this the hour long etch was tried. The SEM images of the etch results of the front side of the membrane and the back side are shown in Figure 4.7 and Figure 4.8 respectively. The size of the etched features on the front side of the membrane versus the back side is shown in Table 4.3. From Table 4.3 by analyzing the size of the etched features on the front and back side, it was evident that the membrane was etched all the way through the nitride.

Table 4.3: Size of the etched features on the front side of the membrane versus the back side.

Etched Features	Front side	Back side
700nm	672nm	684nm
300nm	306nm	322nm
200nm	188nm	206nm
100nm	87nm	91nm

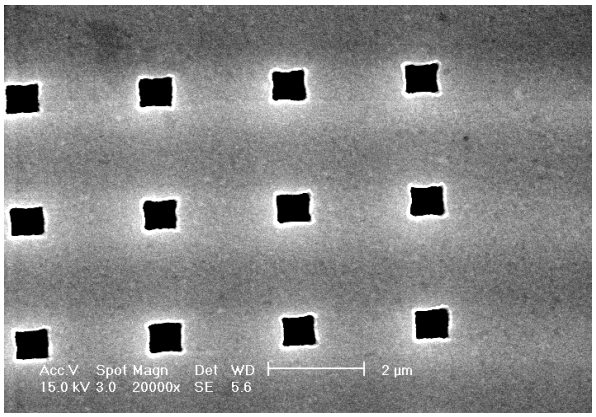

(a)

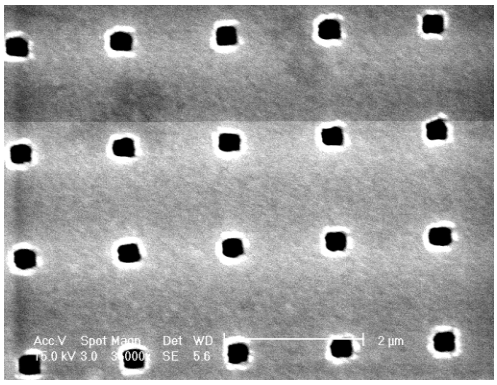

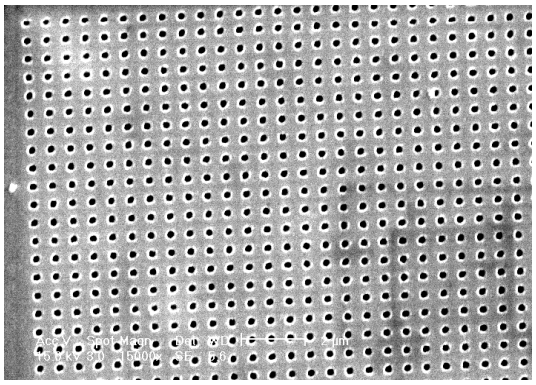

(b) (c)

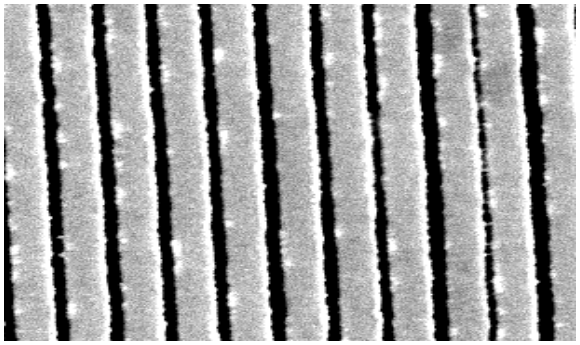

(d)

Figure 4.7: SEM images of front side of a silicon nitride membrane of (a) 700nm (b) 300nm (c) 200nm (d) 100nm features etched through in SF_6 and oxygen for an hour.

.

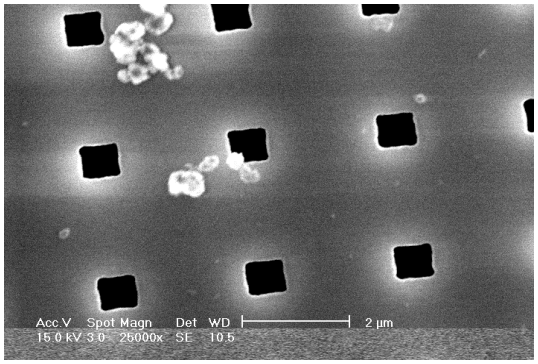

(a)

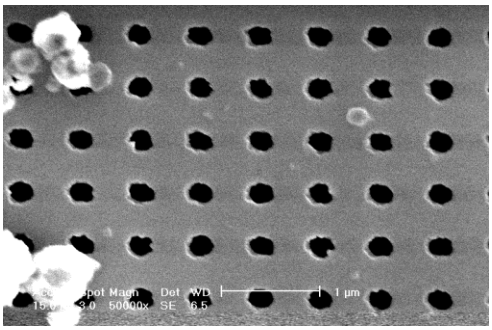

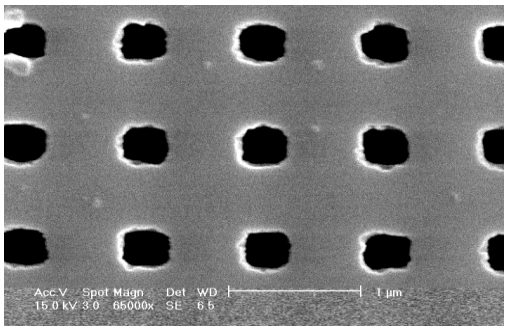

(b) (c)

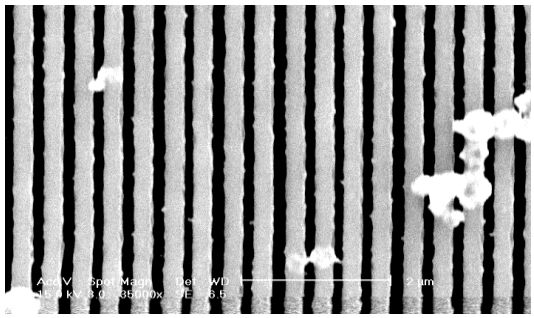

(d)

Figure 4.8: SEM images of back side of a silicon nitride membrane of (a) 700nm (b) 200nm (c) 300nm (d) 100nm features etched through in SF_6 and oxygen for an hour.

4.3.3 Membrane Etching With Metal at the Back

Previous experiments with membrane etching have shown that the center of the membrane etch slowly compared to the edges. The reason being that free standing silicon nitride membranes have very poor thermal conductivity and due to the heat of the plasma generated during the etch, the center of the membrane gets heated up more by thermal conduction compared to the edges. As a result of this heating, the etch process slows down considerably in the center. To overcome this heating effect, a metal with a very thermal conductivity was deposited at the back of the membrane for the reactive ion etch process and was stripped off after the etch was done. Figure 4.9 shows this process.

Figure 4.9: Silicon nitride membrane with (a) no metal and (b) metal at the back.

(a) Using Gold: The metal that was tried in the first place was gold which has a thermal conductivity of $317 Wm^{-1}K^{-1}$. On a membrane with 20nm of copper and 200nm of PMMA, 100nm of gold was deposited on its back side by thermal evaporation. The membrane was exposed to patterns varying from 100nm to 5 microns and developed. The Argon milling step was run for 15 minutes followed

by RIE in 0.8mTorr of SF_6 and 0.2mTorr of oxygen at a power of 15 watts for an hour. The front side images of the membrane were captured by a SEM before removing the gold. The images are in Figure 4.10.

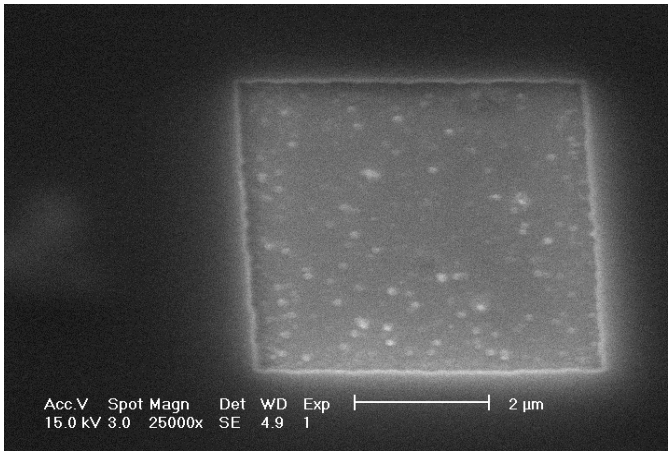

(a)

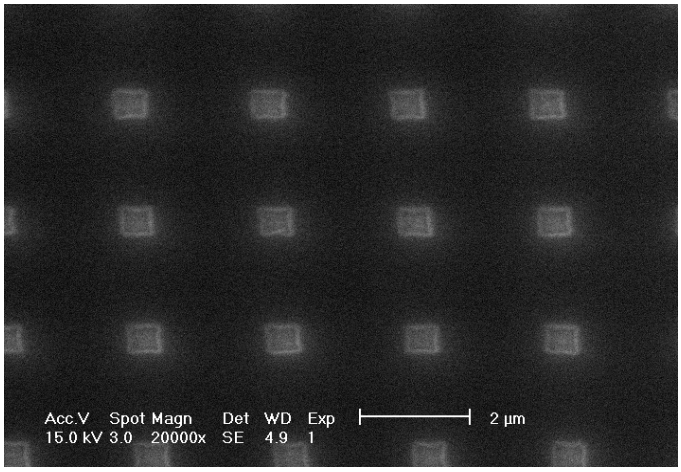

(b)

Figure 4.10: SEM images of front side of a silicon nitride membrane of (a) 5µm (b) 500nm features etched through in SF_6 and oxygen for an hour with 100nm gold at the back.

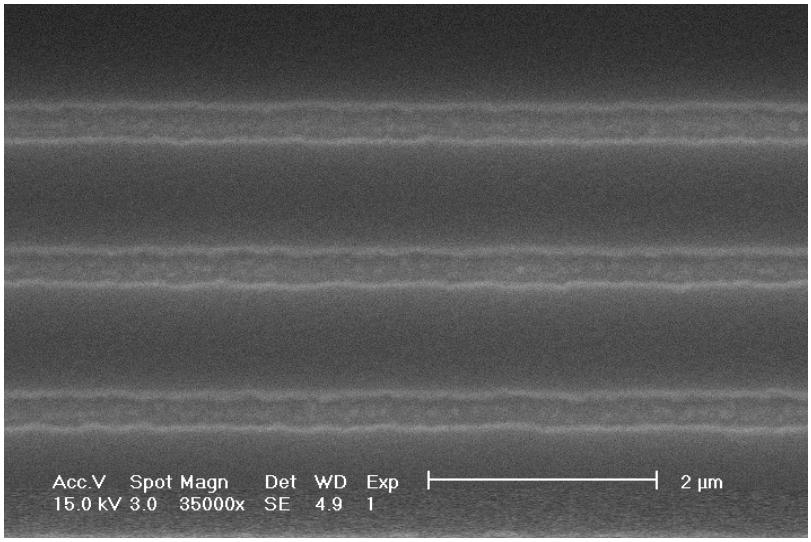

(c)

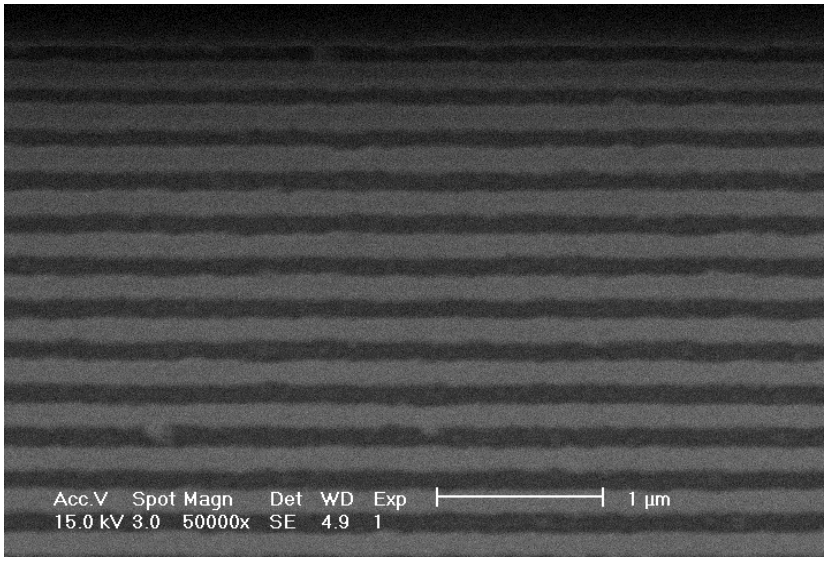

(d)

Figure 4.10: SEM images of front side of a silicon nitride membrane of (c) 300nm (d) 100nm features etched through in SF_6 and oxygen for an hour with 100nm gold at the back (continued).

From these 5 microns, 500nm, 300nm and 100nm features, it was still evident that the edges of these lines were not straight and had a certain degree

of roughness to it. The bright particles visible inside the 5 micron square are basically gold particles. However these were the front side images of the membrane. To view the back of the membrane, the 100nm gold had to be stripped off using Potassium Iodide solution (gold etchant). But the challenge faced during the gold removal step was that the membrane became excessively fragile and flimsy and was broken during the gold etching step. So temporarily the use of gold was withheld and copper was deposited at the back of the membrane as the metal with a high thermal conductivity.

(b) Using Copper: The metal that was tried after gold was copper which has a thermal conductivity of $401 Wm^{-1}K^{-1}$. On a membrane with 20nm of copper and 200nm of PMMA, 100nm of copper was deposited on its back side by thermal evaporation. The membrane was exposed to patterns varying from 100nm to 5 microns and developed. The Argon milling step was for 15 minutes followed by RIE in 0.8mTorr of SF_6 and 0.2mTorr of oxygen at a power of 15 watts for an hour. The front side images of the membrane were taken in the SEM before removing the copper. The images are in Figure 4.11.

From these front side images of the membrane of the 5 microns, 700nm and 200nm features, there were still some roughness observed in the edges. After stripping the 100nm copper in citric acid the back side of the membrane was observed. The SEM images of the back side are in Figure 4.12.

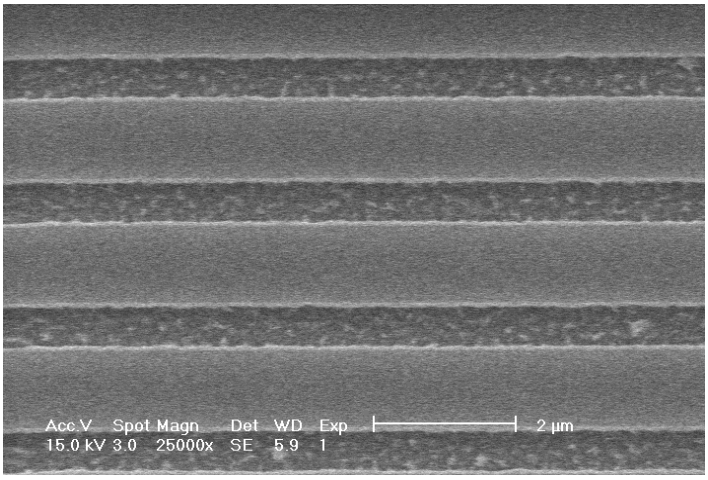

(a)

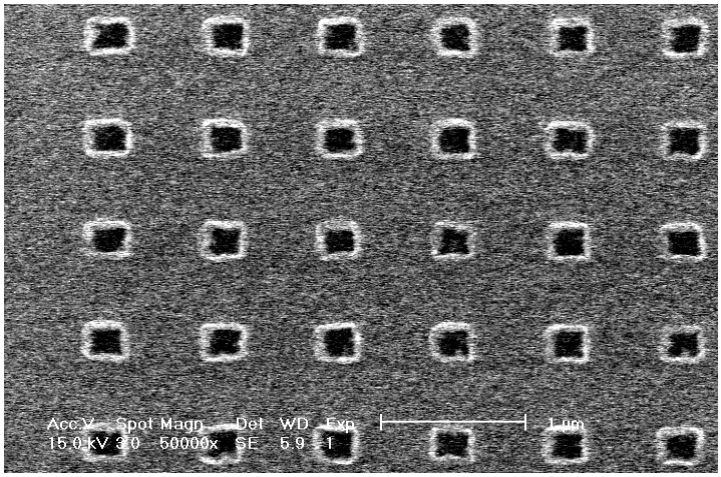

(b)

Figure 4.11: SEM images of front side of a silicon nitride membrane of (a) 700nm (b) 200nm features etched through in SF_6 and oxygen for an hour with 100nm copper at the back.

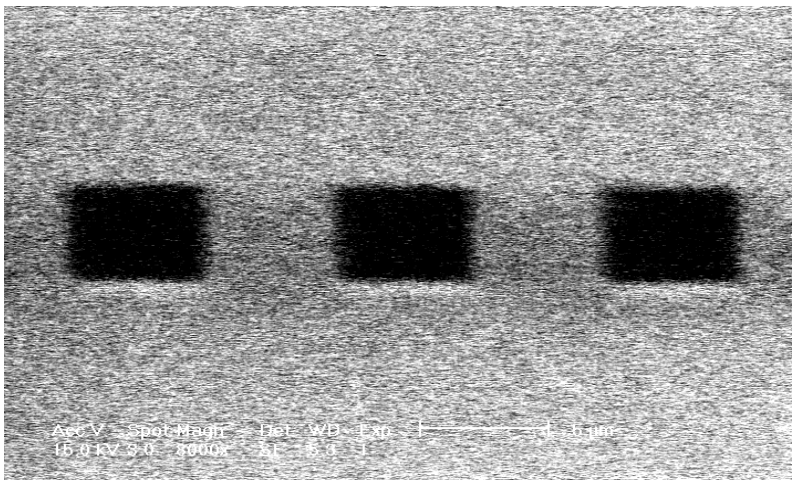

(a)

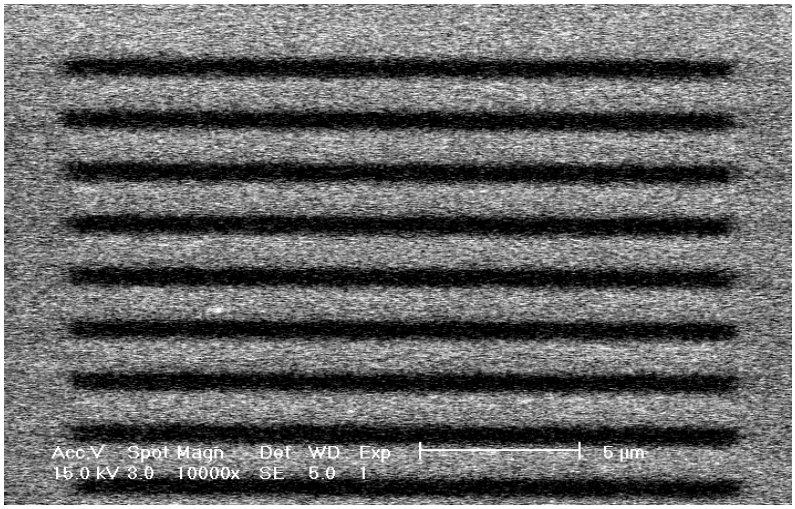

(b)

Figure 4.12: SEM images of back side of a silicon nitride membrane of (a) 5µm (b) 700nm features etched through in SF_6 and oxygen for an hour with 100nm copper at the back.

The excessive roughness from the 5 micron and 700nm images of the back side are due to charging in the SEM. But it can be seen that the back side was etched through however it was still inconclusive when and how long it takes for the center of the membrane to get etched completely.

4.3.4 Uniformity in Membrane Etching

As we have discussed in previous sections, the center of the membrane is heated up by heat of the plasma, and consequently takes longer time to etch than the edges. In the next set of experiments, a membrane of silicon nitride was taken and coated with 20nm of copper and 200nm of PMMA. On this sample, test patterns of 5 micron squares were printed at a pitch of 10 microns over 12mm length and developed. In other words, this was an experiment to find out exactly how long it takes to etch the center of the membrane (at the 6mm mark). An argon mill for 15 minutes at a process pressure of 1mTorr at 13 watts was carried out followed by RIE in 0.8mTorr of SF_6 and 0.2mTorr of oxygen at a power of 15 watts for intervals of 30, 40, 50, 60 and 70 minutes. The images were taken in the optical microscope of the back side of the membrane. This membrane however had no metal coating at its back. It was essential to know how long it takes to etch through the center of the membrane without any metal on its back. The images of the center of the membrane are in Figure 4.13.

From Figure 4.13 (a), (b), (c), (d) and (e) taken at 30, 40, 50, 60 and 70 minutes respectively, it was clear that without any metal at the back it took 70 minutes to etch the center of the membrane completely. The color change in the patterns after the time intervals is clear and after 70 minutes the dark squares demonstrate that the center was etched all the way through. In other words we require a near 250 percent over etch to etch all the way through (it takes roughly 20 minutes to remove 500nm of silicon nitride going by our etch rates).

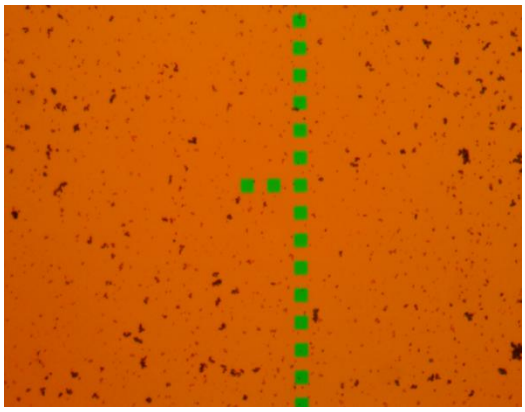

(a)

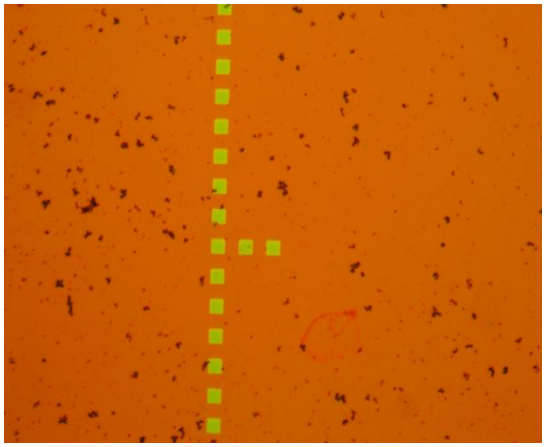

(b)

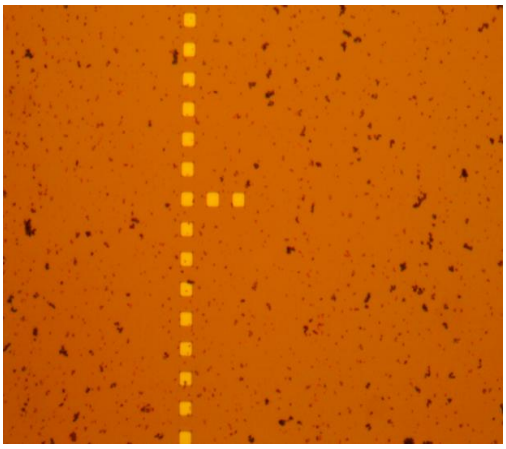

(c)

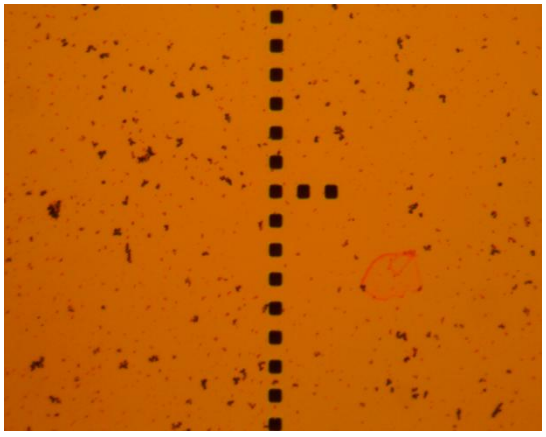

(d)

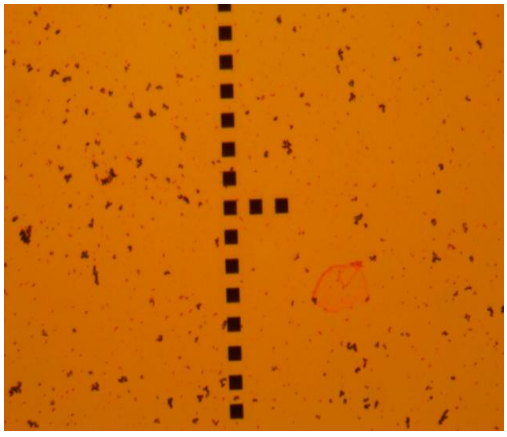

(e)

Figure 4.13: Images of back side at the center of a silicon nitride membrane after (a) 30 minutes (b) 40 minutes (c) 50 minutes (d) 60 minutes (e) 70 minutes of etching in SF_6 and oxygen for an hour without any metal on its back side.

In contrast the edges of the membrane took 40 minutes to etch through completely. The optical microscope images of the edges of the membrane are shown in Figure 4.14 after 40 minutes of RIE in 0.8mTorr of SF_6 and 0.2mTorr of oxygen

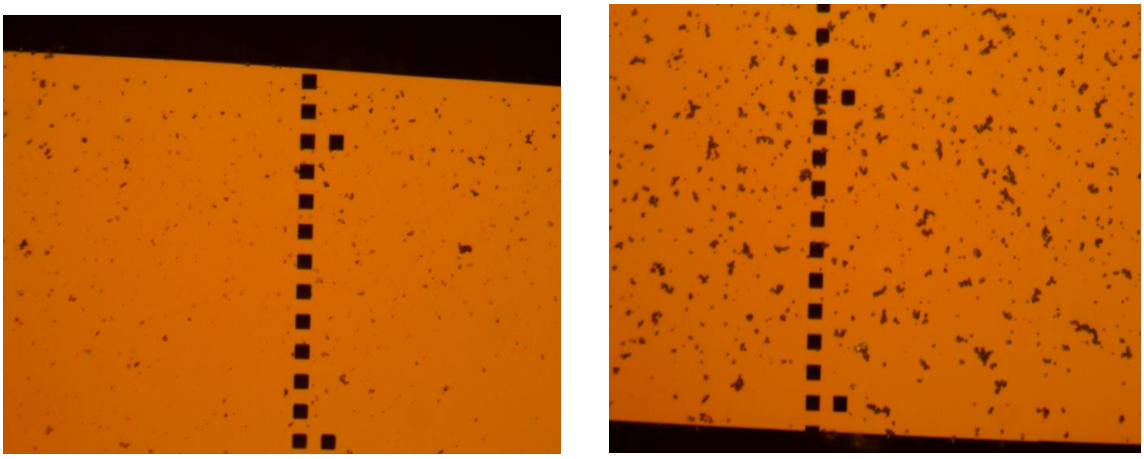

(a) (b)

Figure 4.14: Images of back side at the edges of a silicon nitride membrane at a distance of (a) 1.8mm (b) 11.6mm after etching in SF_6 and oxygen for 40 minutes without any metal on its back side.

These edge images are taken at 1.8mm and 11.6mm respectively for Figure 4.14 (a) and (b). It is clear from the dark squares that the holes are etched completely at the edges after only 40 minutes of RIE, thus justifying the need to use a metal at the back of the membrane to improve etch uniformity throughout the membrane. A graph was plotted between the fractional distance of the etched holes from the edge of the membrane to the center against time (in minutes) shown in Figure 4.15.

From the graph plotted between the fractional distance of the etched holes from the edge of the membrane to the center (in Y-axis) against time (in

minutes on the X-axis), it was seen that 70 minutes was the time it took to clear the openings in the center of the membrane.

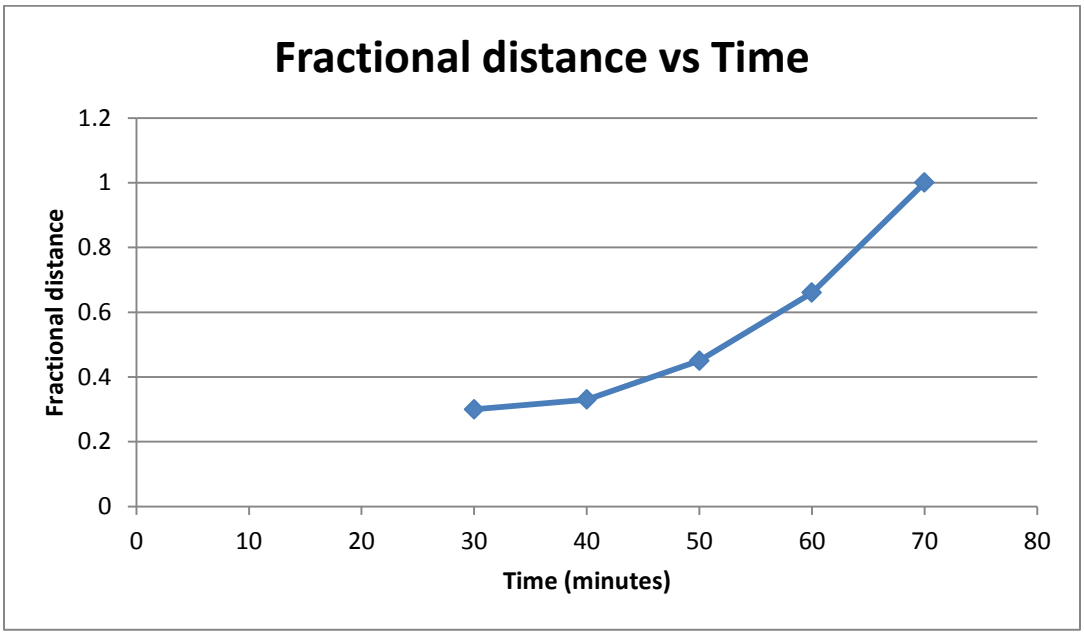

Figure 4.15: Graph between the fractional distance of the etched holes from the edge of the membrane to the center against time (in minutes).

Our next experiment was on a membrane with 100nm of copper on its back. As stated earlier, copper has very high thermal conductivity that is expected to keep the center of the membrane cooler and prevent overheating. So, a membrane with 20nm of copper and 200nm of PMMA on its front side and with 100nm of copper on its back side was used and the 5 micron squares at a pitch of 10 microns over 12mm length were printed and developed. An argon mill for 15 minutes at a process pressure of 1mTorr at 13 watts was carried out followed by RIE in 0.8mTorr of SF_6 and 0.2mTorr of oxygen at a power of 15 watts for 40 minutes before stripping off the 100nm of copper on the back side of

the membrane in citric acid solution. The optical microscope images of the edge and center (6mm mark) of the back side of the membrane are shown in Figure 4.16 after removing the copper at the back.

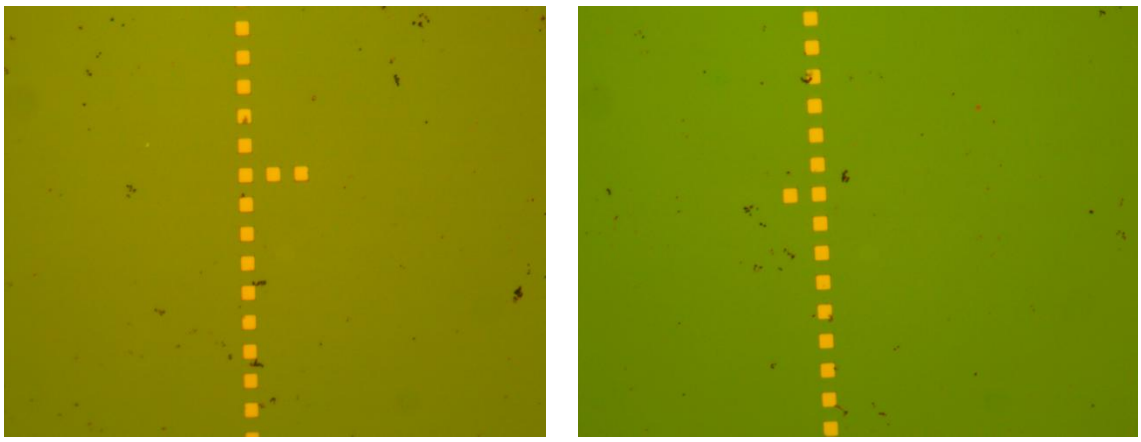

(a) (b)

Figure 4.16: Images of back side of a silicon nitride membrane at a distance of (a) 1.8mm (edge) (b) 6mm (center) after etching in SF_6 and oxygen for 40 minutes after stripping off 100nm copper from its back.

The images in Figure 4.16 (a) and (b) are of the edge of the membrane and center respectively. The colors inside the squares are yellowish green which is perhaps due to a deposition from copper and sulfur. But the point to observe was that the color of the patterns on the edges as well as the center was the same, indicating it might have etched uniformly throughout in 40 minutes of RIE. The only question that remained was the deposited material on these openings that were not clearing off. The process that was tried was bombarding the back of the membrane with argon ions (milling) for 30 minutes but the results observed after this was that the same deposition existed in these openings. We however

can conclude that since the color of these openings were the same throughout the membrane, the uniformity issue that occurred previously due to poor thermal conduction, was taken care of by the metal at the back of the membrane when it was exposed in the heat of the plasma. So 100nm of copper at the back of the membrane can be seen as an alternative to overcome this heating issue associated with membrane etching.

4.3.5 Conclusion

The unreliability associated with the wet was definitely overcome by the dry etching techniques. The biggest advantage of the dry etch process is that it does not suffer from poor photoresist adhesion problems which was in the case of wet etch. Also, the other noticeable thing about the dry etch process is that the etch profile is anisotropic in nature and generally gives straight etch profiles and practically suffers from no undercutting like the wet etch process. The significant challenge faced during this process was the etch uniformity on the membrane due to the center of the membrane getting heated up by thermal conduction. That problem was overcome by depositing a metal with very high thermal conductivity on the back of the membrane (gold and copper tried in this work). Although the openings were covered with some copper and sulfur deposition, the hypothesis was that the patterns were clearly etched all along the membrane quite uniformly as seen from the color of the etched features. Thus, we can conclude that a robust etch process with SF_6 and oxygen to etch the patterns all the way through the nitride membrane has been developed.

Chapter 5 Variation of Etch Rates and Selectivity with Power

The last set of experiments were conducted in order to optimize the entire process by measuring various etch rates of silicon nitride and copper in 0.8 mTorr of SF_6 and 0.2 mTorr of O_2 at various power settings and also calculating the selectivities at those power settings. This was done in order to select the exact power settings for our process. Table 5.1 shows the etch rates of silicon nitride at different power settings.

Table 5.1: The etch rates of silicon nitride at different power settings.

Power (watts)	Rates (nm/min)
10	27
15	30
20	35
25	38
30	40

The etch rates increase with the increase in power settings. The influence of power is straightforward: an increase of power increases both the density and the energy of the free electrons. Therefore, the DC bias voltage becomes more negative with increasing power and the rates of ionization increases leading to an

increase in etch rates. The graphs plotted between etch rates and power setting is shown in Figure 5.1.

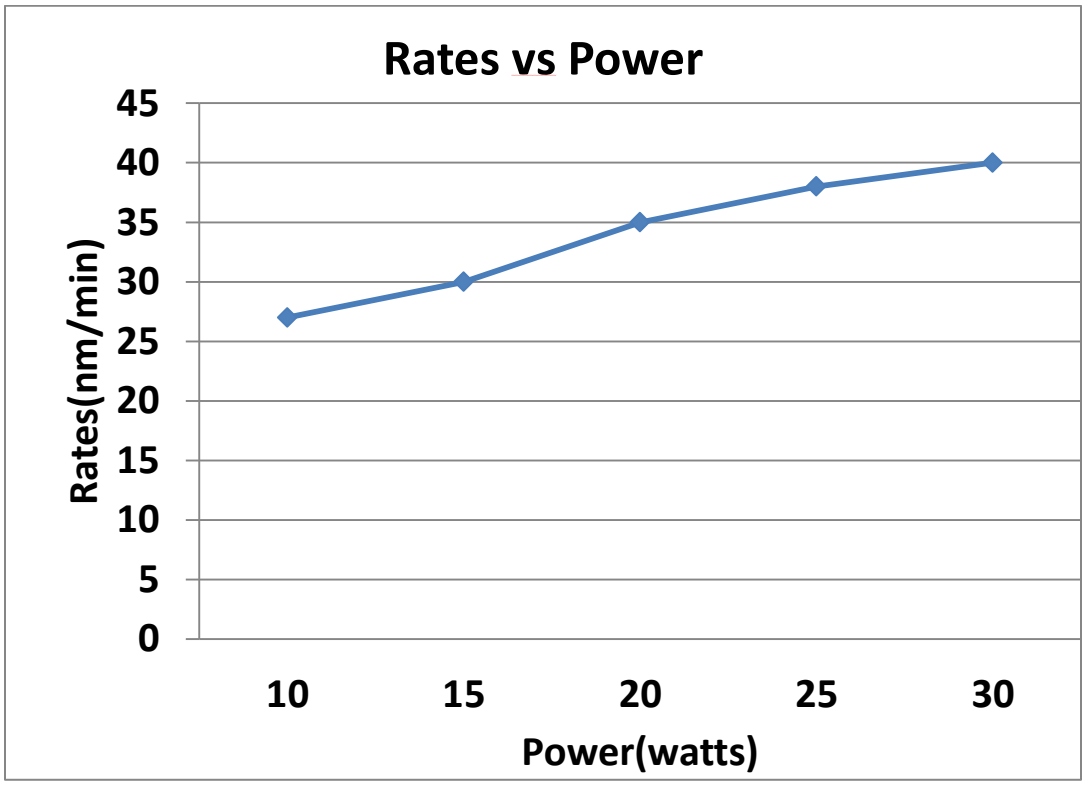

Figure 5.1: Graph plotted between silicon nitride etch rates & power settings.

The copper rates were measured after RIE in 0.8 mTorr of SF_6 and 0.2 mTorr of O_2 at exactly the same power settings as the ones used for the nitride etch rate measurement. Table 5.2 shows the etch rates of copper at different power settings.

Table 5.2: The etch rates of copper at different power settings.

Power (watts)	Rates (nm/min)
10	0.13
15	0.13
20	0.14
25	0.14
30	0.15

Based on these copper rates the selectivity (ratio of the etch rates between the silicon nitride and copper) was measured at these same power settings. Table 5.3 shows the selectivity at the same power settings. The graph plotted between selectivity and power settings in shown in Figure 5.2.

Table 5.3: Selectivity between silicon nitride & copper at different power settings.

Power (watts)	SiNx rates (nm/min)	Copper rates (nm/min)	Selectivity
10	27	0.13	207.7
15	30	0.13	230.8
20	35	0.14	250
25	38	0.14	271.4
30	40	0.15	266.7

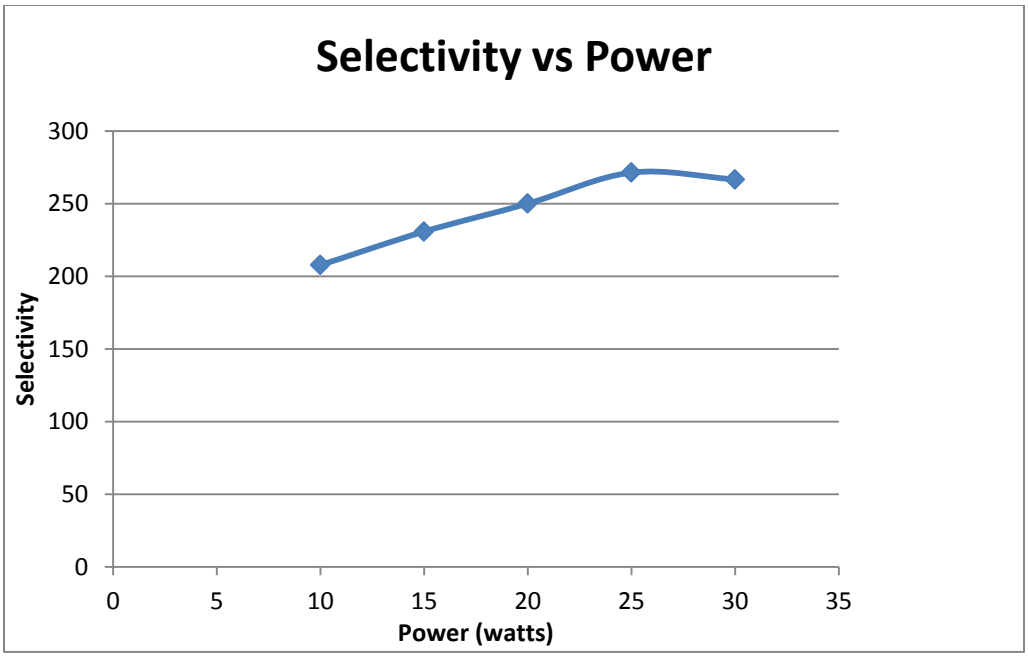

Figure 5.2: Graph plotted between selectivity and power settings.

The selectivity measured is the highest at a power of 25 watts. However in our project the power setting used was 15 watts where the selectivity was 230.8. The reason being that a higher power setting may cause overheating of the membrane and subsequently slow down the process. Thus the power used was 15 watts.

Chapter 6 Summary

In this project, we have successfully developed and optimized a robust dry etch process using argon milling and SF_6 to fabricate silicon nitride stencil masks. Stencil masks are used to print ultra-high resolution patterns using helium ion/atom beam lithography. Several techniques, starting with the wet etch process for mask fabrication, were explored. The main challenge that was encountered was the adhesion issue between PMMA and copper, where the PMMA wasn't sticking to the copper layer underneath and subsequently failed to protect the copper, leading to mask failure. To overcome this unreliability associated with the wet etch, the next process that was explored was the dry etch technique.

The choice of the hard mask was the first critical issue with this process. Experiments proved that copper was the choice for the hard mask over palladium due to the excellent selectivity between silicon nitride and copper in SF_6 and oxygen. The biggest challenge associated with this process was the etch uniformity throughout the membrane due to membrane overheating by thermal conduction. But a potential solution was found out where a metal with high thermal conductivity was deposited at the back of the membrane during the etching steps. Finally the suitable conditions of the process such as the power settings and the variation of the selectivity with different power settings were analyzed in order to optimize the process and sub 200nm features were successfully etched through the masks.

References

[1] A.Nasrullah, “Shape Engineered Nanoparticle Fabrication for Biomedical Applications,” PhD Dissertation, University of Houston, 2011.

[2] J. Randall, D. Flanders, N. Economou, J. Donnelly, and E. Bromley, “Masked ion beam resist exposure using grid support stencil masks,” *Journal of Vacuum Science & Technology B: Microelectronics and Nanometer Structures*, vol. 3, no.1, pp. 58-61, 1985.

[3] S. Pang, M. Geis, W. Goodhue, N. Efremow, D. Ehrlich, R. Goodman, and J. Randall, “Pattern transfer by dry etching through stencil masks,” *Journal of Vacuum Science & Technology B: Microelectronics and Nanometer Structures*, vol. 6, no. 1, pp. 249-252, 1988.

[4] J. Randall, “Pattern distortions in stencil masks,” *Journal of Vacuum Science & Technology B: Microelectronics and Nanometer Structures*, vol. 12, no. 6, pp. 3543-3546, 1994.

[5] J. Randall, L. Stern, and J. Donnelly, “The contrast of ion beam stencil Masks,” *Journal of Vacuum Science & Technology B: Microelectronics and Nanometer Structures*, vol. 4, no. 1, pp. 201-204, 1986.

[6] J. Randall, D. Flanders, N. Economou, J. Donnelly, and E. Bromley, “Silicon nitride stencil masks for high resolution ion lithography proximity printing,” *Journal of Vacuum Science & Technology B: Microelectronics and Nanometer Structures*, vol. 1, no. 4, pp. 1152-1155, 1983.

[7] P.Ruchhoeft, J.C.Wolfe and R.Bass, “Ion Beam aperture-array lithography,” *Journal of Vacuum Science & Technology B: Microelectronics and Nanometer Structures*, vol. 19, no. 6, pp. 2529-2532, 2001.

[8] A. Malinin, T. Majamaa and A. Hovinen, “Anisotropic Si reactive ion etching in fluorinated plasma,” Electron Physics Laboratory, Helsinki University of Technology, 1998.

[9] T.Sherlock, “Fabrication of Micron Scale Retroreflectors for Novel Biosensors,” PhD Dissertation, University of Houston, 2011.

[10] V. Parekh, A. Ruiz, P. Ruchhoeft, H. Nounu, D. Litvinov, and J. C. Wolfe, “Estimation of scattered particle exposure in ion beam aperture array lithography,”*J. Vac. Sci. Technol. B*, vol. 24, no.6, pp. 2915-2919, 2006.

[11] J. Dulak, B. J. Howard, and Ch. Steinbrüchel, “Etch mechanism in the reactive ion etching of silicon nitride,” *J. Vac. Sci. Technol*. *A*, vol. 9, p. 775-778, 1991.

[12] H.Jansen, M.de Boer, J.Burger, R.Legtenberg, M.Elwenspoek, “The Effect of Mask Material and Loading on the Reactive Ion Etching of Deep Silicon Trenches,” MESA Research Institute, University of Twente, 1995.

[13] G.M. Atkinson and N.W. Cheung, “The Effects of Mask Scattering on Photoresist Profiles in Masked Ion Beam Lithography,” Department of Electrical Engineering and Computer Sciences, and the Electronics Research Laboratory, University of California, Berkeley, 1985.

[14] J.C. Wolfe, S.V. Pendharkar, P.Ruchhoeft, S.Sen, M.D. Morgan, “A proximity ion beam lithography process for high density nanostructures,” *J. Vac. Sci. Technol. B* vol.14, no.6, pp.3896-3899, 1996.

[15] F. O. Fong, D. P. Stumbo, S. Sen, G. Damm, D. W. Engler, J. C. Wolfe, J. N. Randall, P. Mauger, and A. Shimkunas, “Low stress silicon stencil masks for sub-100 nm ion beam lithography,” *Microelectronic Engineering,* vol. 11, no. 1-4, pp. 449–452, 1990.